

Polarizational bremsstrahlung in non-relativistic collisions

A. V. Korol^a, A. V. Solov'yov^b ‡

^a Department of Physics, Russian Maritime Technical University, Leninskii prospect 101, St. Petersburg 198262, Russia

^b Frankfurt Institute for Advanced Studies, Johann Wolfgang Goethe-Universität, 60054 Frankfurt am Main, Germany

Abstract. We review the developments made during the last decade in the theory of polarization bremsstrahlung in the non-relativistic domain. A literature survey covering the latest history of the phenomenon is given. The main features which distinguish the polarization bremsstrahlung from other mechanisms of radiation are discussed and illustrated by the results of numerical calculations.

1. Introduction.

In this paper we review recent developments in the theory of polarizational bremsstrahlung (BrS).

Consider the two mechanisms of the photon radiation during a collision shown in figure 1. On the left-hand side of the figure, ordinary BrS (OBrS) is illustrated. In this case the emission of a photon occurs by a charged projectile accelerated in the static field of a target. This is a well known quantum mechanical process the basic description of which can be found in textbooks (see, e.g. [1]). The right-hand picture in the figure illustrates the polarizational BrS (PBrS) [2]. Here, the photon emission occurs due to the virtual excitations (polarization) of the target electrons under the action of the field created by a charged projectile.

The importance and the fundamental character of the OBrS process has been recognized long ago (for a review of historical background see [3]). Since then it has been intensively studied theoretically, numerically and experimentally in a wide range of the projectile and the emitted photon energies, different geometries of the emission, and a variety of atomic and ionic targets. The reviews of the results obtained in this field include [4–8]. The spectral [9] and spectral-angular distributions [10] of OBrS are tabulated over wide ranges of energies of projectile electron and emitted photon and for a number of atomic targets.

‡ On leave from: Ioffe Physical-Technical Institute, Russian Academy of Sciences, St. Petersburg 194021, Russia

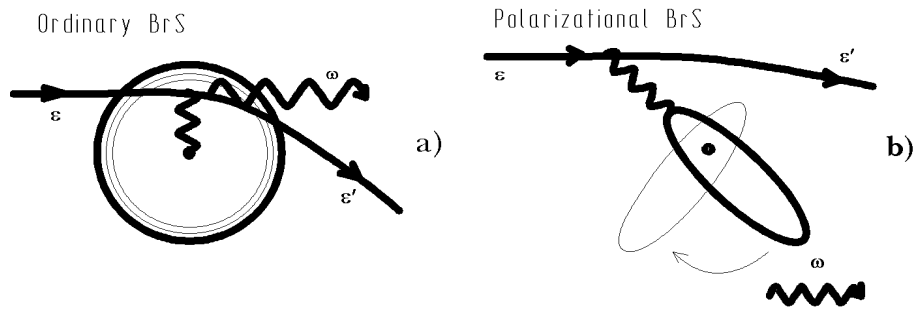


Figure 1. Schematic representation [88] of the ordinary and polarizational BrS processes. Ordinary BrS is the photon emission of a charged projectile accelerated in the static field of the target. Polarizational bremsstrahlung mechanism considers the photon emission of the target electrons, virtually excited by the projectile. Virtual excitation of the electrons is equivalent to polarization of the target.

The polarizational mechanism of the radiation was recognized relatively recently [11–19] where the first qualitative and quantitative estimates were made of the role of the target polarization in forming the BrS spectrum in an electron-atom collision in the range of photon energies close to the atomic ionization potentials.

In the subsequent decade the theory of the effect was developed further and a number of new phenomena was recognized and described both analytically and numerically. An important idea of a close relationship between wide and powerful maxima in experimentally measured emission spectra of electrons [20] and the giant dipole resonances in photoionization of many-electron atoms was formulated [21]. The effect of a dynamic descreening (‘stripping’) of a many-electron subshell for the photon energy larger than its ionization potential was formulated [22] and on its basis the additional asymmetry of the experimentally measured emission spectrum [23] was explained. The numerical calculations of the PBrS spectrum and angular distribution in collisions of electrons with many-electron atoms were performed for fast [24, 25] and intermediate energy [26, 27] projectiles. A formalism and specific features of the dipole-photon polarizational BrS in relativistic collisions of structureless charged particles with atoms were reported [28, 29].

The theory of PBrS in collisions of charged particles, other than electrons, with atoms/ions was developed. In [30] analytical treatment of the exactly solvable problem of the PBrS arising in a positron and a proton collision with a hydrogen atom was given. It was shown that over wide range of the photon energies the BrS intensities for both projectiles are of the same order of magnitude. The PBrS formalism for a bare-ion—atom collision [31, 32] and a bare-ion—hydrogen-ion collision [33] was developed and the performed calculations allowed to explain the earlier measured experimental data on the BrS spectrum of protons. A more general treatment of the BrS arisen in the collision of two complex colliders (atoms, ions), which accounts also for the recoil effect of the nuclei, was carried out in [34, 35].

The important feature of the PBrS mechanism is that it leads to the emission in

collisions of two electrically neutral objects possessing an internal structure. In [34,35] for the first time it was demonstrated that the intensive BrS emission can appear in atom–atom collision. In this case the radiation is due to the mutual virtual polarization of the colliders. The total induced dipole moment of the system alters during the collision, and this results in the photon emission. The general formalism developed in the cited papers allowed to express the BrS amplitude via the generalized atomic polarizabilities of the colliders. It was demonstrated that no dipole photon emission appear in symmetric collisions. The specific features (due to the Coulomb repulsion) of the PBrS formed in ion–ion collision were studied in [36]. The numerical calculations carried out in [34] have shown that the radiation intensity in the collision of two neutral (but different) atoms is comparable to that formed in the collision where one of the colliders is substituted with a charged heavy particle or an electron of the same velocity. Later the formalism, initially developed for non-relativistic atomic collisions, was extended to the relativistic domain [37–39].

For several cases which allow for the exact analytical treatment of the PBrS process the corresponding formulae were derived. These include the PBrS formed in fast electron–hydrogen atom collision [40, 41], in electron/positron collisions with muonic hydrogen [42, 43], and in the collision of a charged particle with positronium [44]. A universal character of the PBrS mechanism, i.e. its (qualitative) independence on the type of the interaction between a projectile and a target was demonstrated in [45, 46] for the processes of neutron– and neutrino–atom scattering (see also the earlier publications [47, 48]). The PBrS manifests itself in nuclear collisions [49], and in nuclear reactions such as α , β , γ decays or nuclear fission process [50].

In the papers [39, 51–53] a theoretical study of the BrS process accompanied by the excitation or ionization of the target (an ‘inelastic’ BrS) was carried out. The photon energy intervals were established where the contribution of the inelastic BrS is small compared to the BrS process without the change in the target’s state.

Some of the results, obtained within the period until the early 90th, were reviewed in [2, 54, 55].

During the last decade a systematic quantitative investigation of the PBrS has been carried out. With the increase of the computer power it has become possible to effectively compute the characteristics of BrS for various projectiles, complex targets (isolated many-electron atoms, atoms in an environment, clusters) and over broad ranges of photon energies. The accurate theoretical predictions on the magnitude of the BrS cross sections, obtained over ranges of energies and targets accessible to experiment [56–59], become available. The combination of theoretical and numerical tools has allowed not only to analyze and test different schemes used to describe the scattering process and the dynamic response of the target (these are two key elements of the PBrS process) but to develop alternative methods as well.

A general approach to consider the BrS process (both the ordinary and the polarizational) in collisions with many-electron targets is based on a consistent application of quantum mechanics and quantum many-body theory. The main results

obtained by using this approach include: (a) application of the many-body theory for accurate calculations of the dynamic generalized polarizability of the target [60–64] (b) development of the methods for approximate treatment of the dynamic response of the target [65–70], (c) calculation of the total BrS spectra of in collisions of non-relativistic electrons on many-electron atoms over wide range of emitted photon energies including the regions of giant resonances [71–74], (d) theoretical description of the PBrS in collisions of slow atomic particles and in collisions involving atoms in the excited states [75–77], (e) numerical calculations of inelastic BrS [78, 79], (f) theoretical and numerical description of the BrS process in electron-cluster collisions [80–84], (g) the full relativistic description of the BrS in a charged particle–atom collision [85–87].

Some of the results presented in the papers cited above were reviewed by us some time ago [88]. In full the results obtained by means of the quantum-mechanical description during the whole period of the PBrS history were summarized in the book [89] (in Russian). Thus, the motivation for writing the current review is to present the results obtained in our group during the latest period for a wider community. In what follows we focus on the achievements made in the development of the theory of PBrS formed in non-relativistic collisions of various particles with isolated many-electron atoms. We also included the part devoted to the BrS formed in atom–atom collisions. The reason for this is that although these results were obtained nearly twenty years ago [34, 35] they have not been reviewed in international journals. The specific features of the polarizational BrS process in electron-cluster collisions and those due to the relativistic effects in electron-atom collisions are not included in this paper but are discussed in other reviews in this issue [90, 91].

During the last decade another approach to the BrS problem (with both channels included) has been developed for theoretical and numerical description of the process in collision with isolated atoms and in plasma [92–98]. It is based on a semi-classical description of the scattering process and the ordinary BrS channel [99], whereas the dynamic atomic response is calculated within the local density approximation. These results were reviewed recently [100, 101], and are not discussed in detail in the present paper.

Other issues which are left beyond the scope of this review include the influence of the density effect on the PBrS for energetic projectiles penetrating through dense medium [102–106] and the multiphoton PBrS [92, 107–110].

The atomic system of units is used.

2. Main features of the polarizational bremsstrahlung process.

In this section we review the peculiar features of polarizational BrS which distinguish this mechanism from ordinary BrS and which manifest themselves in the spectrum of the total BrS. Focusing on the physical nature of these phenomena and to avoid unnecessary complexities, we consider the BrS process of a non-relativistic charged structureless particle on a many-electron target (called an atom, for brevity) within the framework of

the plane-wave first Born approximation for the scattering process and the dipole-photon scheme for the description of the photon-atom and photon-projectile interactions. Such treatment, although quite often being insufficient for the quantitative description of the process, allows one to carry out a simple qualitative analysis and to explain all specific features of PBrS.

Let \mathbf{p}_1 and \mathbf{p}_2 denote the momenta of initial and final states of the projectile with mass m and charge e . To simplify the formalism we consider the BrS process in the collision with a spherically symmetric neutral atom. This restriction is not too rigid since the effects described below also occur in the BrS process on a target with a ground state of arbitrary symmetry.

Considering the two mechanisms of the photon emission one derives the following expression for the total amplitude of the process:

$$f_{\text{tot}} = f_{\text{ord}} + f_{\text{pol}} = \frac{4\pi(\mathbf{e}\mathbf{q})}{q^2} \left[\frac{e^2}{m} \frac{Z - F(q)}{\omega} + e\omega\alpha(\omega, q) \right], \quad (1)$$

where \mathbf{e} and ω are the photon polarization vector and energy, $\mathbf{q} = \mathbf{p}_1 - \mathbf{p}_2$ is the momentum transfer.

The first term in (1) describes the ordinary part of the total amplitude. It is proportional to $Z - F(q)$, where $F(q)$ is the form-factor of atomic electrons and Z is the charge of the nucleus. Hence, f_{ord} is dependent on the static distribution of the charge in the atom. The polarizational amplitude f_{pol} is expressed via a generalized atomic dynamic polarizability $\alpha(\omega, q)$ which appears as a result of the action of two field on the atom: the field of the projectile and the electromagnetic field of the emitted photon.

The first feature which distinguishes between the two mechanisms follows immediately from (1). The amplitude of ordinary BrS is inversely proportional to the mass of projectile, while the polarizational part is independent of it. The explanation for this fact follows from the basic principles of electrodynamics (e.g. [1]). During the process of ordinary BrS, it is the projectile that emits the photon. The intensity of this radiation is proportional to the square of the projectile acceleration in the external field of a target. In turn, the acceleration is proportional to $1/m$ and this dependence manifests itself in f_{ord} . In contrast, during the polarizational BrS the projectile serves as a source of the external field acting on the atomic electrons, and thus the amplitude of this process is almost insensitive to the variations of m [2]. Moreover, the intensity of PBrS for a heavy projectile is comparable and can be even higher than that of an electron of the same velocity [34].

Other qualitative differences between the two mechanisms of the photon emission one can trace by comparing the dependencies of f_{ord} and f_{pol} on the photon energy and on the momentum transfer.

The OBrS amplitude is a smooth function of ω . The only peculiarity appears in the soft-photon region $\omega \rightarrow 0$ where a simple perturbative approach, giving an infinite magnitude of f_{ord} , fails to describe the process. This phenomenon, known as the "infrared catastrophe", had been recognized and understood long ago [1]. The q dependence of f_{ord} is concentrated in the factor $Z - F(q)$. The atomic form-factor $F(q)$

is the Fourier image of the electron charge distribution and is a monotonically decreasing function of q . Qualitatively, the value $F(q)$ defines the number of atomic electrons inside the sphere of a radius $r \sim 1/q$. Hence, this function reaches its maximum value at $q = 0$ where $F(0) = Z$ and decreases monotonically with the increase of q . In the case of large q , $\lim_{q \rightarrow \infty} F(q) = 0$. The natural scale to measure the magnitude of q is the inverse radius of the target, R_{at}^{-1} . Thus, the amplitude of OBrS is large for $q > R_{\text{at}}^{-1}$ while in the region $q \ll R_{\text{at}}^{-1}$ it becomes negligibly small. Such behaviour has a clear explanation [5]. To radiate a photon via the ordinary mechanism a projectile must penetrate inside the atom, at a distance $r < R_{\text{at}}$, where a strong nuclear potential $-Z/r$ is less screened by the electron cloud. In the opposite limit, when $r \gg R_{\text{at}}$, the nucleus is fully screened by the electrons (in the case of a neutral target) and the probability for a projectile to get the acceleration and to radiate vanishes.

The PBrS appears as a result of the alteration of the atomic dipole moment induced during the collision. There are two external fields - the field the photon and the Coulomb field of the projectile - which act on the atom in this process. The dynamic response of the target depends, therefore, on the parameters of both fields. Formally, it is reflected in the dependence of the generalized dynamic polarizability $\alpha(\omega, q)$ on two variables. We use the term 'generalized' when addressing to $\alpha(\omega, q)$ in order to stress the dependence on q , and, thus, to distinguish this quantity from the dipole dynamic polarizability, $\alpha_{\text{d}}(\omega)$, to which $\alpha(\omega, q)$ reduces in the limit of small transferred momenta:

$$\lim_{q \rightarrow 0} \alpha(\omega, q) = \alpha_{\text{d}}(\omega). \quad (2)$$

The dependence on q appears because of the action of the external Coulomb field of the projectile. This field distorts the electrons' orbits and induces a dipole moment of the atomic system. The dipole polarization of the electron cloud is most pronounced if the Coulomb field of the projectile is uniform on the scale of R_{at} , i.e. when the projectile is outside the target, $r \gg R_{\text{at}}$. These distances correspond to small values of the transferred momentum $q \ll R_{\text{at}}^{-1}$ where, in accordance with (2), the PBrS amplitude, as well as the cross section, can be expressed through $\alpha_{\text{d}}(\omega)$. For small distances, $r \ll R_{\text{at}}$, the field of the projectile is almost spherically symmetric. Therefore, it induces a small dipole moment on the target. Hence, in contrast to the ordinary BrS process, it is the large distances between the projectile and the target which are of the most importance for the PBrS mechanism [17, 21].

The ω dependence of $\alpha(\omega, q)$ reflects the ability of the electron cloud to be dynamically polarized by an external electromagnetic field of a given frequency. In a many-electron atom the electrons are distributed among the atomic subshells. Each subshell is characterized by an ionization potential I . In terms of classical mechanics this corresponds to the frequency of the rotation of electrons of a given subshell around the nucleus. Using this analogy one may say that the dynamic response of the electron cloud to the external field increases for those ω which are close to the ionization thresholds of the target subshells. Therefore, in the region

$$I_1 < \omega < I_{1s}, \quad (3)$$

where I_1 and I_{1s} stand, respectively, for the ionization potentials of the outermost shell and of the $1s$ shell, the function $\alpha(\omega, q)$ is non-monotonic with extrema in vicinities of the ionization potentials.

This happens, in particular, when the photon energy lies within the region of a giant dipole resonance of the photoionization cross section of a many-electron atomic subshell [111]. For the first time wide maxima in the emission spectra were observed experimentally in electron scattering from (solid) Ba, La and Ce [112, 113]. Later these were explained theoretically [16] by relating the maxima to the virtual excitations of the $3d$ -subshell electrons. In [20] a powerful maximum was observed in the emission spectrum in electron-La collision. In the subsequent paper [21] for the first time an important conclusion was drawn about the common nature of the giant resonances in photoionization and those in PBrS spectra. To reveal this similarity one recalls that at large distances between the projectile and the atom the amplitude of the PBrS process is proportional to the dipole dynamic polarizability, $\alpha_d(\omega)$. The imaginary part of this quantity is related to the photoionization cross section $\sigma_\gamma(\omega)$ through (e.g. [114]):

$$\text{Im } \alpha(\omega) = \frac{c}{4\pi\omega} \sigma_\gamma(\omega), \quad (4)$$

where $c \approx 137$ is the velocity of light. Since the OBrS amplitude is real (see (1)), the modulus square of the imaginary part of f_{pol} enters the total BrS cross section as an additive term. Therefore, a maximum in $\sigma_\gamma(\omega)$ manifests itself in the BrS spectrum as well reflecting the collective nature of the dynamic response of atomic electrons.

Although based on the assumption that main contribution to f_{pol} comes from the region of large distances $r \gg R_{\text{at}}$, which does not always lead to a correct quantitative result, the qualitative arguments of [21] provided a clear physical explanation of the nature of powerful maxima in emission spectra. The experiments, carried out later, supported the theoretical prediction. The maxima in the BrS spectra were measured for Ba and several rare-earth elements [115, 116], for La and for atoms from the lanthanum group [117], for Xe [23, 118] and for Ba [56]. In all these experiments, performed for various energies of the incoming electron (ranging from several hundreds of eV up to several keV), the powerful BrS maxima were observed for photon energies within the ranges of the giant resonances in the photoionization cross section of the $4d$ subshells.

The existence of the maxima in the BrS spectrum due to a strong effect of polarization of many-electron atomic subshells was confirmed by a number of independent theoretical calculations [22, 24–27, 34, 60, 61, 63, 66, 68] which were carried out within the frameworks of various models.

In general, in the whole ω -region defined by (3), a highly non-monotonic behaviour of the generalized polarizability of a many-electron atom results in a series of peculiarities (maxima, minima, cusps) in the total BrS spectrum. The important role of the polarizational mechanism in forming the total BrS spectra over a wide range of photon energies was analyzed in [71–73, 77, 119].

For the photon energies noticeably higher than the $1s$ ionization potential, $\omega \gg I_{1s}$, the ω dependence of $\alpha(\omega, q)$ is much like that for the cloud of free electrons. The leading

term in the expansion of $\alpha(\omega, q)$ in powers of ω/I_{1s} reads:

$$\alpha(\omega, q) \approx -\frac{F(q)}{\omega^2}. \quad (5)$$

As a result, for a fast electron ($m = 1$, $e = -1$) the total amplitude reduces to the BrS amplitude on a bare nucleus [15]:

$$f_{\text{tot}} \approx \frac{4\pi(\mathbf{e}\mathbf{q})}{q^2} \frac{Z}{\omega}. \quad (6)$$

This shows that for large ω the atomic electrons do not participate in the screening of the nucleus and do not contribute to the BrS cross section. Thus, in the region $\omega \gg I_{1s}$ the polarizational channel results in a (dynamic) de-screening of the nucleus.

The physical reason for this effect (following [22] we use the term ‘stripping’ effect) is that, for $\omega \gg I_{1s}$, the electrons of all atomic subshells may be treated as free ones [15]. If the incident electron is also free (the Born approximation) then there is no dipole radiation by a system of free electrons.

These arguments allow one to construct an approximate expression for the total BrS amplitude for photon energies lower than the $1s$ -shell ionization threshold [22]. For a fixed value of ω the target electrons can be divided into two groups, the ‘inner’ and the ‘outer’ electrons. The former are those whose binding energies, I_{in} , exceed ω , and, therefore, their orbits are not distorted noticeably by an external electromagnetic field of a frequency ω . Hence, the inner electrons do not contribute to the amplitude of the PBrS. The outer electrons have the binding energies I_{out} less than ω . Under the action of the field they behave as free electrons, and their contribution to f_{pol} can be described by (5) where $F(q)$ must be substituted with the form-factor of the outer electrons, $F_{\text{out}}(q)$. As a result the total BrS amplitude acquires the form

$$f_{\text{tot}} \approx \frac{4\pi(\mathbf{e}\mathbf{q})}{q^2} \frac{Z - F_{\text{in}}(q)}{\omega}, \quad (7)$$

where $F_{\text{in}}(q)$ stands for the form-factor of the inner electrons. This expression demonstrates that the outer electrons do not participate in the screening of the nucleus (or, in other words, the nucleus is ‘stripped’ by a total number N_{out} of the outer electrons). The physical reason for this partial ‘stripping’ is as formulated above: for $\omega \gg I_{\text{out}}$ the outer electrons can be considered as free and, therefore, there is no dipole-photon emission by the system ‘projectile electron + the outer electrons’.

Although the ‘stripping’ approximation does not account for the specific details of the PBrS amplitude near each subshell threshold, it allows one to estimate the behaviour of the smooth background of the BrS cross section curve. In particular, on its basis the asymmetry of the giant resonances in the experimentally measured emission spectra [23,115,117] was explained. Namely, from (7) follows that the difference between two values of the function ωf_{tot} calculated for (a) $\omega \gg I_j$ (I_j is the ionization potential of the j th subshell), and for (b) $\omega \ll I_j$, is proportional to the form-factor $F_j(q)$ of the subshell which can be estimated as $F_j(q) \approx N_j$, where N_j is the number of the electrons in the subshell. Therefore, the difference between the two amplitudes is proportional to N_j , and the increase in the cross section is $\sigma(\omega \gg I_j) - \sigma(\omega \ll I_j) \propto N_j^2$ [22].

This qualitative explanation was confirmed by numerical calculations [24] carried out within the framework of the non-relativistic Born approximation. Later the 'stripping' was generalized, going beyond the Born approximation [65, 70, 120].

When the photon energy becomes small compared with the first ionization potential of the target one can expect the decrease of the contribution of the polarizational BrS channel into the total spectrum. From (1) follows that for $\omega \ll I_1$ the PBrS amplitude behaves as $f_{\text{pol}} \propto \omega \alpha(0, q) \sim \omega \alpha_{\text{d}}$, where α_{d} is a static dipole polarizability of the target. In contrast, the OBrS term increases. For the ratio of the two terms $f_{\text{pol}}/f_{\text{ord}} \sim m\omega^2 \alpha_{\text{d}}/e$ vanishes as ω goes to zero. For low but non-zero values of ω the contribution of the polarizational channel strongly depends on the magnitude of the static polarizability. The higher the magnitude of α_{d} is, the wider is the ω interval where the contribution of f_{pol} might be noticeable.

These arguments are valid also beyond the range of validity of the first Born approximation, on the basis of which (1) was derived. In the low-frequency limit the OBrS amplitude is expressed in terms of the amplitude of elastic scattering, $f_{\text{ord}} \propto f_{\text{el}}/\omega$ (e.g., [114]). On the other hand, the process of PBrS occurs most effectively at large distances between the projectile and the target, where the wavefunction of the projectile is not affected strongly by the potential, and one can use the Born approximation to describe the polarizational channel even for low-energy projectiles. Therefore, the ratio of the two amplitudes still is proportional to $\omega^2 \alpha_{\text{d}}$. In [18] the role of the polarizational channel was studied in the inverse BrS process (i.e. BrS absorption) for slow electrons scattered from atoms. It was demonstrated that for an e^- -Ar scattering the polarizational mechanism changes noticeably the absorption coefficients, whereas for an e^- -Ne scattering its influence is much less. This quantitative effect is due to large difference in the static polarizabilities: $\alpha_{\text{d}}^{\text{Ar}} = 11.10$ a.u. and $\alpha_{\text{d}}^{\text{Ne}} = 2.66$ a.u. [121]. Rather strong effect of the target polarization on the BrS spectra was reported recently [122] for low-energy ($\varepsilon_1 = 0.4 \dots 3.5$ eV) electron-rare-gas atom collisions.

In general, in the collisions of slow heavy particles with atoms both the ordinary and the polarizational mechanisms fail to describe adequately the radiation spectrum. In such processes another mechanism, known as molecular orbital radiation, becomes important (see, e.g., [123]). Nevertheless, the polarizational BrS is important in asymmetric slow collisions of atoms and ions in the region of large impact parameters [75]. The intensity of the OBrS is negligibly small due the large masses of the colliders.

However, the situation with the radiation formed in the slow charged particle-excited hydrogen collision is somewhat different, compared with PBrS and also with molecular orbital radiation. More accurately, in addition to these types of radiation there is a peculiar source of low-frequency photon emission [76]. In this case the radiation is generated by the rotating dipole moment of the hydrogen during the collision. The specific feature of the hydrogen atom introduces the linear Stark effect (see, e.g., [124]). The electric field of the projectile splits the initially degenerated levels of the excited hydrogen. Atomic states with a given principal number form a Stark multiplet. The components of the multiplet already possess a dipole moment. The vector of this dipole

moment rotates following the movement of the projectile, and the radiation appears as a result of this rotation. We stress that this mechanism of BrS is intrinsic for systems with a linear Stark effect. This is also a distinguishing feature from the ‘real’ PBrS which also appears because of the alteration of the target’s dipole moment. In the latter case it is really the induced dipole moment intrinsic for systems with a quadratic Stark effect. As a result the character of these spectra at low frequencies are quite different [76].

Once the internal dynamic structure of a target is taken into account, the next logical step is to consider the radiative processes which are accompanied by the excitation or ionization of the target. Following [51] we call BrS processes of this type ‘inelastic’ BrS contrary to the ‘elastic’ one, when the target remains in its ground state after the collision. Within the framework of the same approximations as above the amplitude of the scattering process accompanied by the real atomic transition from the initial ground state 0 to the final state m may be written as follows:

$$f_{\text{tot}}^{(m)} = f_{\text{ord}}^{(m)} + f_{\text{pol}}^{(m)} = \frac{4\pi}{q^2} \left[-\frac{\mathbf{e}\mathbf{q}}{\omega} \frac{e^2}{m} F_{m0}(\mathbf{q}) + e\omega A_m(\mathbf{e}, \omega, \mathbf{q}) \right]. \quad (8)$$

Here $F_{m0}(\mathbf{q}) = \langle m | \exp(i\mathbf{q}\mathbf{r}) | 0 \rangle$ is a non-diagonal form-factor and the function $A_m(\mathbf{e}, \omega, \mathbf{q})$ is defined as

$$A_m(\mathbf{e}, \omega, \mathbf{q}) = \sum_n \left\{ \frac{\langle m | \mathbf{e}\hat{\mathbf{p}} | n \rangle F_{n0}(\mathbf{q})}{\omega_{nm} - \omega - i0} + \frac{F_{mn}(\mathbf{q}) \langle n | \mathbf{e}\hat{\mathbf{p}} | 0 \rangle}{\omega_{n0} + \omega - i0} \right\}, \quad (9)$$

where the sum is carried out over the whole set of virtually excited states of the target, n , ω_{nm} and ω_{n0} are the transition energies, $\hat{\mathbf{p}}$ is the momentum operator. In the case $m = 0$, i.e. the elastic BrS, this function reduces to $(\mathbf{e}\mathbf{q}) \alpha(\omega, q)$ in accordance with (1).

It is important to establish the contribution of inelastic channels to the total emission spectrum. This is not purely of theoretical interest since experimentally it is quite difficult to separate elastic and inelastic channels. To do this it is necessary to observe the final state of the target with simultaneous detection of the photon.

It has been demonstrated that over a wide region of the photon frequencies, the elastic channel dominates over the inelastic one in the total BrS spectrum for both heavy [51, 53] and light [52, 53] projectiles scattered on a many-electron atom. Semi-quantitatively, the cross sections of the elastic BrS, of both the ordinary and the polarizational nature, exceed those of the inelastic by a factor Z . The explanation is as follows [51, 52]. During the elastic BrS the contributions of each atomic electron to the polarizational part of the total amplitude (1) are coherent, as in Rayleigh scattering of light. Considering the case of a neutral atom and having in mind that the ordinary part of the elastic BrS spectrum is approximately proportional to the nuclear charge squared, one finds that the total elastic cross section is proportional to Z^2 . In contrast, during the inelastic BrS the contributions of each electrons must be summed in the cross section rather than in the amplitude (8). Hence, the inelastic BrS cross section is proportional to Z and is parametrically small in the case of a many-electron target, when $Z \gg 1$.

The region of the photon frequencies, in which the above mentioned coherence effect plays an essential role, is estimated as [51–53]

$$I_1 < \omega < \frac{v_1}{R_{\text{at}}} \quad (10)$$

where v_1 is the initial velocity of projectile. Beyond the region of coherence inelastic BrS becomes more important. An exception of this rule occurs in collisions of fast heavy charged particles with atoms/ions collisions (as well as in atom-atom, ion-atom and ion-ion) in the region of high photon frequencies. In this region the process of inelastic BrS has a threshold, which is equal to $\omega_{\text{max}} \approx v_1^2/2$. However, the elastic BrS takes place at higher energies, up to $\omega \geq 2v_1^2$, dominating in this region in the total photon emission spectrum. Therefore, the photon energy range $v_1^2/2 \leq \omega \leq 2v_1^2$ is convenient for the observation of the elastic PBrS. We note that in this ω region there is a peculiar feature in the spectrum of PBrS [79] similar to that which occurs in inelastic scattering, where it is known as the Bethe ridge [124]. In more detail we discuss this phenomenon in section 4.

The numerical comparison of the relative role of elastic and inelastic channels in proton-atom collisions was performed in [79, 96].

In electron/positron–many-electron atom scattering elastic BrS dominates parametrically over the inelastic one in the region (10). However, if one is interested in accurate data on the total BrS cross section it is necessary to include the inelastic channels into the computational scheme. Up to now, mostly due to technical difficulties, numerical investigations of the role of inelastic BrS have not been as extensive as in the elastic case. The achievements in this field include the model theoretical study carried out in [118, 125] in connection with the experimental data on the intensity of the BrS spectrum in $e^- + \text{Xe}$ collision as a function of the incoming electron energy ε_1 [118, 126] (see also [127, 128] for the experimental data in $e^- + \text{Ar}$ collision).

For low- Z targets the absolute magnitudes of both terms from (1), f^{ord} and f^{pol} , and the terms $f_{\text{ord}}^{(m)}$ and $f_{\text{pol}}^{(m)}$ from (8) are all of the same order. In this case, it is the charge of the projectile which introduces peculiarities in the total radiative spectrum. It can be shown that, both for high frequencies of the photon, $\omega \gg v_1/R_{\text{at}}$ [30, 51] and for the low ones, $\omega \ll 1$ [51, 78] the role of inelastic channels is negligibly small compared with the elastic BrS in the case of electron scattering, while for the positron-atom collision the situation is the opposite. It occurs mainly because of the difference in the behaviour of the interference between the ordinary and polarizational amplitudes in inelastic BrS. The interference is negative in the case of the electron projectile and positive in the positron case. The simplest way to trace this effect is to consider the inelastic BrS amplitude (8) in the limit of high photon frequencies, as was done above for elastic BrS. For $\omega \gg I_{1s}$ the polarizational inelastic amplitude reduces to $f_{\text{pol}}^{(m)} \approx -(4\pi e/q^2) (\mathbf{e}\mathbf{q}/\omega) F_{m0}(\mathbf{q})$. Using this result in (8) one notices that for a projectile electron ($e = -1$) the ordinary and polarizational terms cancel each other out, while for a positron ($e = +1$) the effect is opposite.

To conclude this part of the paper we review the theoretical approaches used to

describe the BrS process in non-relativistic collisions. These can be subdivided into three parts: (a) methods applied to analyze the scattering process, (b) models used to describe the interaction with the photon, and (c) the approximations used to describe the dynamic atomic response.

The variety of theoretical approaches used to describe the scattering process range from the first-order plane-wave Born approximation to more sophisticated ones. Since the OBrS phenomenon has much longer history these methods were first tested in application to this process and later on were used in the PBrS problem. In application to the BrS problem in electron-atom scattering the models beyond the plane-wave Born approximation, used in both the non-relativistic and the relativistic domains include the corrections due to the Elwert factor and its modifications [120, 129, 130], the use of Sommerfeld-Maue functions [114, 129], the approaches based on the use of classical [131, 132] and semi-classical [99, 100] theories. The best available results have been obtained using the distorted partial-wave expansion of the projectile wavefunction. This scheme has been applied to study the ordinary BrS process of non-relativistic projectiles in the dipole-photon approximation [133, 134]. The most adequate description of the process has been obtained by applying the DPWA and using the multipole expansion for the projectile-photon interaction operator [135–138].

In many papers on the PBrS problem the non-relativistic Born approximation was used for both light (a positron, an electron) and heavy (a proton, an ion) projectiles. Although the range of validity of the Born approximation for PBrS is larger than for OBrS, to obtain more accurate data on the total BrS cross sections of a light projectile it is necessary to go beyond this scheme. Therefore, the non-relativistic DPWA formalism was developed [26, 27, 60, 139, 140] and applied to calculate the cross sections $d\sigma$ and $d^2\sigma$ over a broad spectral range [61, 63, 71–73, 77, 119] for non-relativistic electrons scattered on many-electron atoms. The partial-wave approach was also used to study the PBrS process of slow electrons [18, 19, 141, 142].

In most of the papers the dynamic atomic response to the joint actions of the field of the projectile and of the radiation field was treated within the frame of the non-relativistic dipole-photon theory (with exception for several papers mentioned below). Even within this framework the accurate calculation of the generalized polarizability $\alpha(\omega, q)$ is not a simple task. Apart from the case of a hydrogen atom (or hydrogen-like ion) where the analytical evaluation is possible [11, 40, 77] one has to use more sophisticated approaches to calculate this quantity. The methods known to us include the the Hartree-Fock based calculations with [22, 24, 25, 60–63, 66, 72] and without [26] the inclusion of many-body corrections, the approach based on the local-density approximation (see [100] and references therein). Another semi-empirical approach for effective and quite accurate calculation of $\alpha(\omega, q)$ for complex systems was proposed recently [66–68]. This method as well as the approach [69] based on the use of the non-relativistic Coulomb Green function and valid for the calculation of $\alpha(\omega, q)$ in the vicinities of K- and L-shells are described in sections 3 and 4.

Beyond the dipole-photon approximation the PBrS was considered in collisions of a

non-relativistic heavy projectile with many-electron atom [29, 37, 38, 143, 144]. In these papers the corrections of the order $kR_{\text{at}} \ll 1$ were considered and it was demonstrated that they lead to the additional modification of the angular distribution of the radiation. More systematic analysis of the non-dipolar corrections has become available recently within the framework of the full relativistic description of the PBrS process [85, 86].

In what follows we discuss in some more the formalism related to the PBrS problem and present the results of numerical calculations of the BrS spectrum to illustrate the main features of the process described above.

3. Bremsstrahlung of electrons on atoms.

The differential cross section, which characterizes the spectral distribution of the radiation, is given by

$$\begin{aligned} d\sigma_{\text{tot}}(\omega) &\equiv \omega \frac{d\sigma_{\text{tot}}}{d\omega} = \frac{\omega^4}{(2\pi)^4 c^3} \frac{p_2}{p_1} \sum_{\lambda} \int d\Omega_{\mathbf{p}_2} \int d\Omega |f_{\text{tot}}|^2 \\ &= d\sigma_{\text{ord}}(\omega) + d\sigma_{\text{pol}}(\omega) + d\sigma_{\text{int}}(\omega). \end{aligned} \quad (11)$$

The integration is carried out over the directions of propagation of the scattered particle ($d\Omega_{\mathbf{p}_2}$) and the emitted photon ($d\Omega$), the summation is over the photon polarizations. In a general case, the amplitude f_{tot} includes the ordinary and the polarizational parts. Therefore, there are three terms appearing in the cross section of the process. In (11) $d\sigma_{\text{ord}}(\omega) \propto |f_{\text{ord}}|^2$ and $d\sigma_{\text{pol}}(\omega) \propto |f_{\text{pol}}|^2$ stand for the cross sections of the OBrS and PBrS processes, and $d\sigma_{\text{int}}(\omega)$ is the interference term proportional to $\text{Re}(f_{\text{pol}}^* f_{\text{ord}})$. Note that $d\sigma_{\text{int}}(\omega)$ can be of either sign. In the case of a heavy projectile the ordinary BrS can be neglected and, thus, $f_{\text{tot}} \approx f_{\text{pol}}$ and $d\sigma_{\text{tot}}(\omega) \approx d\sigma_{\text{ord}}(\omega)$. For a light projectile it is necessary to retain all the terms in the amplitude and the cross section.

In this section we consider the case of electron-atom scattering. An adequate description of the BrS emission formed in the intermediate energy electron-atom collision is obtained by using the distorted partial-wave approximation (DPWA) [26, 140]. In the lowest order of the non-relativistic perturbation theory in the electron-dipole-photon interaction and in the Coulomb interaction $\hat{V} = \sum_a |\mathbf{r} - \mathbf{r}_a|^{-1}$, between the incident (\mathbf{r}) and atomic (\mathbf{r}_a) electrons (the sum is carried out over all atomic electrons), the amplitudes f_{ord} and f_{pol} are given by the expressions:

$$f_{\text{ord}} = \langle \mathbf{p}_2^{(-)} | \mathbf{e}\mathbf{r} | \mathbf{p}_1^{(+)} \rangle \quad (12)$$

$$f^{\text{pol}} = - \sum_n \left[\frac{\langle 0 | \mathbf{e}\mathbf{D} | n \rangle \langle \mathbf{p}_2^{(-)} | n \rangle \langle \hat{V} | \mathbf{p}_1^{(+)} | 0 \rangle}{\omega - \omega_{n0} + i0} - \frac{\langle \mathbf{p}_2^{(-)} | 0 \rangle \langle \hat{V} | \mathbf{p}_1^{(+)} | n \rangle \langle n | \mathbf{e}\mathbf{D} | 0 \rangle}{\omega + \omega_{n0}} \right], \quad (13)$$

where $|\mathbf{p}_1^{(+)}\rangle$ and $|\mathbf{p}_2^{(+)}\rangle$ are the wavefunctions of the incident and the scattered electrons with asymptotic momenta \mathbf{p}_1 and \mathbf{p}_2 , respectively. The ‘ \pm ’ superscripts correspond to the out- (‘ $+$ ’) and to the in- (‘ $-$ ’) scattering states, the DPWA expansions of which is

$$|\mathbf{p}_j^{(\pm)}\rangle = 4\pi \sqrt{\frac{\pi}{p_j}} \sum_{lm} i^l \exp(\pm i\delta_l(p_j)) \frac{P_{\nu_j}(r)}{r} Y_{lm}^*(\mathbf{p}_j) Y_{lm}(\mathbf{r}). \quad (14)$$

Here $\delta_l(p)$ are the phaseshifts, the notation ν stands for a set of quantum numbers (p, l) . The radial wave functions $P_\nu(r)$ satisfy the Schrödinger equation with the ‘frozen’ core.

Vector \mathbf{D} in (13) is the operator of the dipole interaction of the atomic electrons with the electromagnetic field, $\omega_{n0} = E_n - E_0$ is the energy of the atom’s transition from the ground state 0 to the virtually excited state n (including excitations into the continuum).

The PBrS amplitude can be expressed in terms of the generalized dynamic polarizability $\alpha(\omega, q)$. Omitting the details (see [60]) we present the result:

$$f_{\text{pol}} = \frac{1}{2\pi^2} \int d\mathbf{Q} \frac{e\mathbf{Q}}{Q^2} \langle \mathbf{p}_2^{(-)} | e^{-i\mathbf{Q}\mathbf{r}} | \mathbf{p}_1^{(+)} \rangle \alpha(\omega, Q), \quad (15)$$

where the integration is carried out over the entire space of the vector \mathbf{Q} . This form of representation provides a straightforward reduction to the Born limit of f_{pol} . Indeed, substituting the distorted waves $|\mathbf{p}_{1,2}^{(\pm)}\rangle$ with the wavefunctions for a free particle, $|\tilde{\mathbf{p}}_{1,2}^{(\pm)}\rangle = \exp(i\mathbf{p}_{1,2}\mathbf{r})$ one derives the expression for f_{pol} within the framework of the plane-wave Born approximation (see the second term on the right-hand side of 1).

Using the DPWA series (14) in (12), (15) and then in (11) one derives the partial-wave series for the cross section $d\sigma_{\text{tot}}(\omega)$:

$$d\sigma_{\text{tot}}(\omega) = \frac{32\pi^2}{3} \frac{\omega^4}{c^3 p_1^2} \sum_{l_1 l_2} l_{\text{max}} |R_{l_2 l_1}^{\text{ord}} + R_{l_2 l_1}^{\text{pol}}|^2, \quad (16)$$

where $l_2 = l_1 \pm 1$ in accordance with the dipole selection rules, and $l_{\text{max}} = \max\{l_1, l_2\}$. The partial amplitudes of ordinary, $R_{l_2 l_1}^{\text{ord}}$, and polarizational, $R_{l_2 l_1}^{\text{pol}}$, BrS are defined as follows:

$$R_{l_2 l_1}^{\text{ord}} = \langle \nu_2 || r || \nu_1 \rangle \quad (17)$$

$$R_{l_2 l_1}^{\text{pol}} = -\frac{2}{\pi} \int_0^\infty dQ Q \langle \nu_2 || j_1(Qr) || \nu_1 \rangle \alpha(\omega, Q). \quad (18)$$

Here $j_1(Qr)$ is the spherical Bessel function. The notation $\langle \nu_2 || A || \nu_1 \rangle$ is used for the radial integral $\int_0^\infty dr P_{\nu_2}(r) A P_{\nu_1}(r)$.

If one neglects the partial PBrS amplitude $R_{l_2 l_1}^{\text{pol}}$ on the right-hand side of (16) the resulting formula coincides with the known partial-wave expansion for OBrS [133, 134, 145].

The only characteristic in (15) and (18) which depends on the internal dynamics of the target is the generalized polarizability. However, it is exactly the calculation of this quantity which brings a main difficulty in the case of a many-electron target, where an accurate account for many-electron correlations is essential. In [66–68] a simple approximate method was introduced for the calculation of $\alpha(\omega, Q)$ and consequently of $d\sigma_{\text{pol}}(\omega)$. This method allows one to avoid the rather complicated direct numerical computations of the many-electron correlation effects. In short, the method can be described as follows. Let us define a function $G(\omega, q)$ equal to the ratio $\alpha(\omega, q)/\alpha_d(\omega)$ of the *exact* generalized and dipole polarizabilities:

$$\alpha(\omega, q) = \alpha_d(\omega) G(\omega, q). \quad (19)$$

Now let us assume that all the information about the many-electron correlation effects is contained in the dipole polarizability $\alpha(\omega)$, while the factor $G(\omega, q)$ is not that sensitive to them and can be calculated in the simpler approximation, for example within a Hartree-Fock scheme. Then, instead of (19) one can write the following approximate formula:

$$\alpha(\omega, q) \approx \alpha_d(\omega) \frac{\alpha^{\text{HF}}(\omega, q)}{\alpha^{\text{HF}}(\omega)} \equiv \alpha_d(\omega) G^{\text{HF}}(\omega, q). \quad (20)$$

This relation is the key to the method. The approximate equality in (20) reduces a complex problem of the exact computation of $\alpha(\omega, q)$ to a much simpler one: the calculation of the factor $G^{\text{HF}}(\omega, q)$ in the Hartree-Fock approximation. In the papers [60,61,66–68] the validity of this method was checked against more rigorous calculations (carried out within various RPA-based schemes) of $\alpha(\omega, q)$ and $d\sigma_{\text{pol}}(\omega)$ for electron scattering on Ba, La, Eu. The BrS spectrum was calculated in the vicinity of the 4d-subshells ionization potentials where the polarizational mechanism leads to the powerful maximum in the spectrum. Recently this approach was used in [119] to calculate, in a broad range of photon energies, the total BrS spectra in e^- -Kr and e^- -La collisions. In the cited paper the function $G(\omega, q)$ (more exactly, its inverse Fourier image, $G(\omega, r)$) was calculated, following [96], within the local spin density approach.

Another effective method for the approximate calculation of $\alpha(\omega, q)$ in the ω -range close to the ionization thresholds of the K- and L-shells of many-electron atoms was introduced in [69]. It is based on the use of the Coulomb Green function and the hydrogen-like wave functions for the inner shell electrons. In more detail this method is described in section 4.

As was mentioned in section 2 the computation of the dynamic response of the target is simplified considerably if one uses the ‘stripping’ approximation. The latter within the DPWA scheme can be introduced as follows [74]. Using the arguments which lead to (7), one divides the atomic electrons into two groups, the ‘inner’ and the ‘outer’ electrons, following the rule $I_{\text{out}} < \omega < I_{\text{in}}$. Assuming the strong inequality $\omega \ll I_{\text{in}}$, one can neglect the contribution of the virtual excitations of the inner electrons to the sum in (13). Then, the amplitude f_{pol} can be approximated by the contribution of the outer-shell electrons alone:

$$f_{\text{pol}} \approx - \sum_{a,a'=1}^{N_{\text{out}}} \sum_n \left[\frac{\langle 0 | \mathbf{e} \mathbf{r}_a | n \rangle \langle \mathbf{p}_2^{(-)} n | v_{a'} | \mathbf{p}_1^{(+)} 0 \rangle}{\omega - \omega_{n0} + i0} - \frac{\langle \mathbf{p}_2^{(-)} 0 | v_{a'} | \mathbf{p}_1^{(+)} n \rangle \langle n | \mathbf{e} \mathbf{r}_a | 0 \rangle}{\omega + \omega_{n0}} \right], \quad (21)$$

where N_{out} is the number of such electrons, and $v_{a'} = |\mathbf{r} - \mathbf{r}_{a'}|^{-1}$.

Assuming the strong inequality $\omega \gg I_{\text{out}}$ as well, one expands the denominators in powers of the small parameter $\omega_{n0}/\omega \sim I_{\text{out}}/\omega$ and evaluates the leading term, proportional to ω^{-2} , with the help of closure $\sum_n |n\rangle \langle n| = 1$:

$$f_{\text{pol}} \approx \frac{1}{\omega^2} \langle \mathbf{p}_2^{(-)} | \mathbf{e} \mathbf{a}_{\text{out}} | \mathbf{p}_1^{(+)} \rangle, \quad (22)$$

where \mathbf{a}_{out} is the acceleration due to the static field of the outer electrons.

To obtain the final expression for f_{tot} let us introduce the operator of the total acceleration \mathbf{a} of the electron in the field of the atom, $\mathbf{a} = -Z\mathbf{r}/r^3 + \mathbf{a}_{\text{in}} + \mathbf{a}_{\text{out}}$,

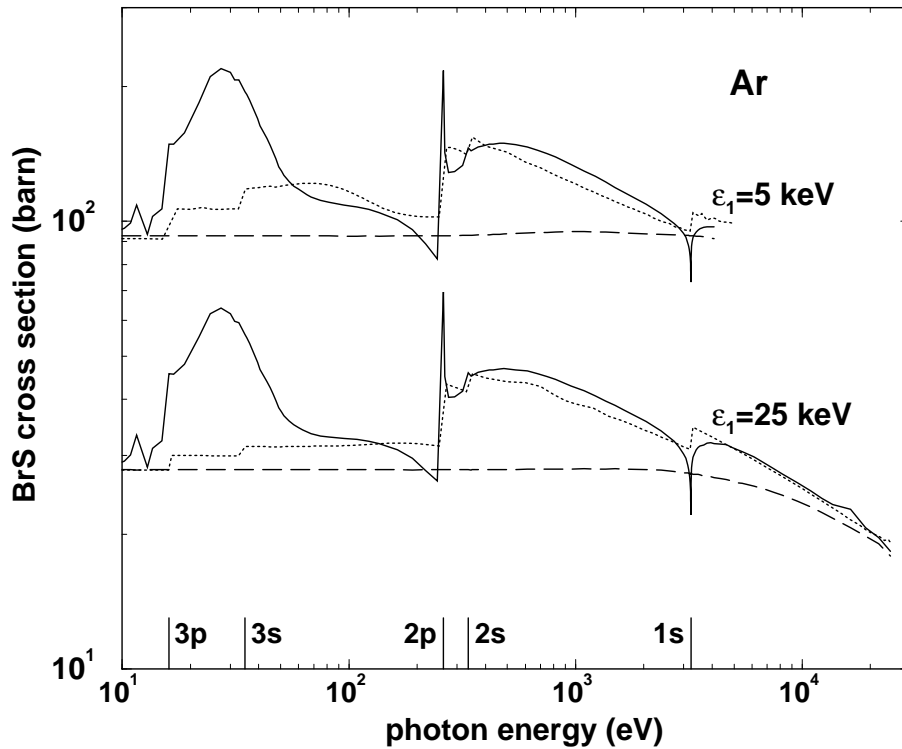


Figure 2. BrS spectra, $d\sigma(\omega)$, formed in collision of $\varepsilon_1 = 5$ keV and $\varepsilon_1 = 25$ keV electrons with an Ar atom. Solid curves represent $d\sigma_{\text{tot}}(\omega)$ within the DPWA and with $\alpha(\omega, q)$ calculated within the RPAE [71]. Dashed curves describe $d\sigma_{\text{ord}}(\omega)$, the dotted lines correspond to the ‘stripping’ approximation (23) [74]. Vertical lines mark the non-relativistic Hartree-Fock ionization potentials of the atomic subshells. See also explanations in the text.

where \mathbf{a}_{in} is the acceleration due to the potential created by the inner electrons. With the help of the relation between the dipole matrix elements in the ‘length’ and ‘acceleration’ forms (see, e.g., [145]), the OBrS amplitude (12) can be cast in the form $f_{\text{ord}} = -\omega^{-2} \langle \mathbf{p}_2^{(-)} | \mathbf{e} \mathbf{a} | \mathbf{p}_2^{(+)} \rangle$. Taking into account equation (22), one obtains the following approximate formula for the total amplitude,

$$f_{\text{tot}} \approx -\frac{1}{\omega^2} \langle \mathbf{p}_2^{(-)} | \mathbf{e} \mathbf{a}_{\text{eff}} | \mathbf{p}_1^{(+)} \rangle, \quad (23)$$

where $\mathbf{a}_{\text{eff}} = -Z \mathbf{r}/r^3 + \mathbf{a}_{\text{in}}$ is the effective acceleration.

Substituting in (23) the distorted waves $|\mathbf{p}_{1,2}^{(\pm)}\rangle$ with the plane waves $\exp(i\mathbf{p}_{1,2}\mathbf{r})$ one derives the formula (7) for f_{tot} within the framework of the plane-wave Born and the ‘stripping’ approximations.

Figures 2 and 3, where the data on the BrS cross sections are presented for 5 and 25 keV electrons scattered on Ar and Xe atoms, illustrate the statements made above.

It is clearly seen that the polarizational mechanism plays an important role in the formation of the total BrS spectrum. Instead of smooth curves, typical for $d\sigma_{\text{ord}}(\omega)$ (the dashed lines), the total BrS curves (the solid lines) exhibit complicated dependence on ω which is characterized by wide powerful maxima and narrow cusps in the vicinity

of the ionization thresholds. Such a behavior is totally due to the contribution of the polarizational, $d\sigma_{\text{pol}}(\omega)$, as well as the interference, $d\sigma_{\text{int}}(\omega)$, terms to the total BrS spectrum.

The total cross section was obtained from eqs. (16)-(18). To calculate the generalized polarizability $\alpha(\omega, q)$ for each value of ω and q we used the random-phase approximation with exchange [111] accounting for the virtual excitations from all atomic subshells. In this sense we may say that the solid lines represent the ‘exact’ $d\sigma_{\text{tot}}(\omega)$.

The powerful maxima in vicinity of the 3p and 3s subshells in the case of Ar, $\omega = 20 \dots 40$ eV, and the 4d and 4p subshells for Xe, $\omega = 80 \dots 110$ eV, appear mainly due to the contribution of the dipole excitations from these subshells to $\alpha(\omega, q)$ and have essentially collective nature. (This is also true for $\omega \sim I_{5p}, I_{5s}$ in figure 3 but in this case the maxima are much less pronounced.) The most part of the intensity radiated in these maxima comes from the imaginary part of $\alpha(\omega, q)$, i.e. is directly related to the corresponding maxima in the photoionization cross section (see the discussion in the paragraph containing eq. (4)). This conclusion becomes more evident if one compares, in these ω ranges, the ‘exact’ BrS spectra with those obtained within the ‘stripping’ approximation, the dotted lines. Within the framework of the ‘stripping’ approximation, eqs. (21) and (22), the imaginary part of the PBrS amplitude is ignored. Meanwhile, it is exactly the imaginary part of f_{pol} which is related to the cross section of photoionization (see (15) and then eqs. (2) and (4)). Therefore, the discrepancy between the solid and the dotted curves in the vicinity of maxima is largely due to the contribution of $\text{Im}(f_{\text{pol}})$.

Apart from the resonant regions the ‘stripping’ approximation reproduces quite well the behaviour of the ‘exact’ curves. The saw-like character of the dotted curves at the thresholds clearly illustrates the physics which is behind this approximation. Namely, for ω larger than an ionization potential I the total BrS cross section increases, because the atom is ‘stripped’ by a total number N of the electrons in the subshell, and, therefore, the field acting on the projectile is stronger than in the case $\omega < I$. In the formal terms the increase in the cross section is due to the change of the sign of the interference term $d\sigma_{\text{int}}(\omega)$ as ω passes through the threshold: $d\sigma_{\text{int}}(\omega)$ is negative for $\omega < I$ and positive beyond the threshold. These arguments explain also the additional asymmetry of the giant resonances in the BrS spectrum and that in the spectrum of photoionization: in the former case the positiveness of the term $d\sigma_{\text{int}}(\omega)$ slows down the decrease of the peak.

In figure 4 the dependences $d\sigma_{\text{pol}}(\omega)$ are presented for ω lying in the region of the giant resonances associated with the excitations from the 4d subshells in Ba, La and Eu. The incoming electron energy is $\varepsilon_1 = 250$ eV.

This figure illustrates two main features of the polarizational BrS. The first one, already mentioned, is the close relationship between the giant resonances in $d\sigma_{\text{pol}}(\omega)$ and those in σ_γ . We note, however, that in general case, the quantity σ_γ associated with the photoabsorption process rather than with the photoionization one alone. The former accounts not only for the ionization into the continuum but the discrete excitations as well. In those cases when excitations into the continuum dominate in the

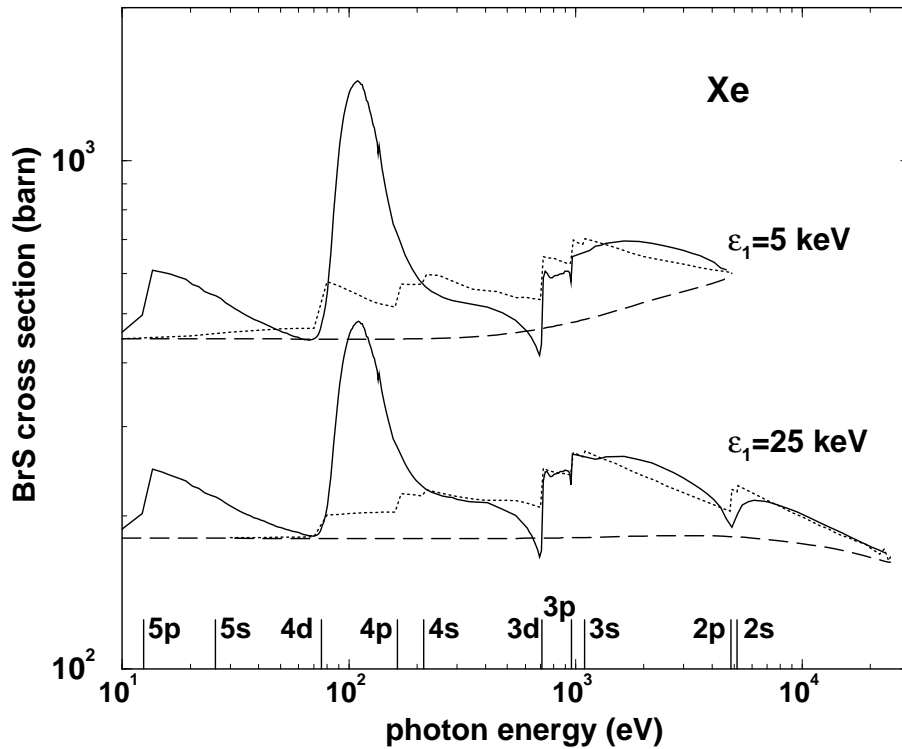


Figure 3. Same as in figure 2 but for a Xe atom.

photoabsorption spectrum the maximum of σ_γ lies above the ionization threshold and so does the maximum of $d\sigma_{\text{pol}}(\omega)$. In connection with figure 4 this is true for Ba and La, and does not hold in the case of a Eu atom. For the latter it is known [146] that the main oscillator strength of the 4d subshell is associated with the discrete transition 4d \rightarrow 4f. Therefore, the maxima of σ_γ and $d\sigma_{\text{pol}}(\omega)$ are located below I_{4d} .

The solid lines in figure 4 were obtained within the DPWA scheme with the partial amplitudes of PBrS computed from (18). The dashed lines correspond to f_{pol} within the Born approximation (see eq. (1)). In both cases to calculate the generalized dynamic polarizability we used the RPAE with relaxation scheme [111] for Ba and La, and the spin-polarized RPAE [147] for Eu.

It is seen that for incident energies as low as 250 eV the Born approximation gives almost the same result as the DPWA. The reason for this coincidence lies in the fact that, in contrast to the process of ordinary BrS, polarizational radiation is formed mainly at large distances, $r \sim p_1/\omega$, between a projectile and an atom [18,21], where the distorting influence of the atomic potential on the projectile's movement is comparatively small. Hence, to calculate the polarizational component of the BrS spectrum, one may use the Born approximation, which results in the formula

$$d\sigma_{\text{pol}}^{\text{B}}(\omega) = \frac{16}{3} \frac{\omega^4}{c^3 p_1^2} \int_{q_{\text{min}}}^{q_{\text{max}}} \frac{dq}{q} |\alpha(\omega, q)|^2, \quad (24)$$

where $q_{\text{min}} = p_1 - p_2$, $q_{\text{max}} = p_1 + p_2$. From a computational viewpoint this expression

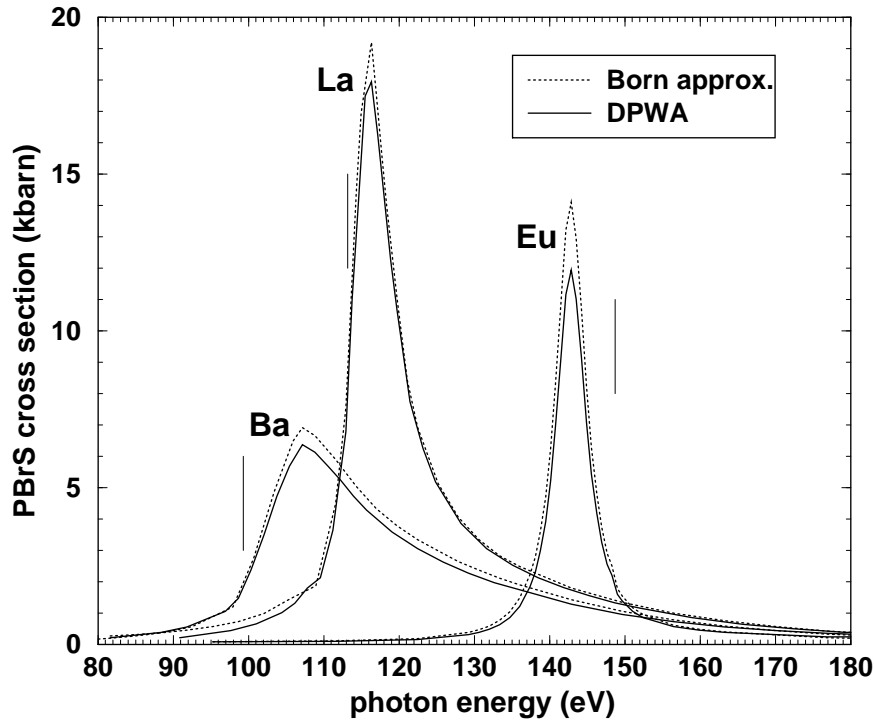


Figure 4. Polarizational BrS cross section $d\sigma_{\text{pol}}(\omega)$ in the vicinity of the 4d ionization potentials (marked with vertical lines). The incident electron energy $\varepsilon_1 = 250$ eV [62].

can be evaluated with much less efforts than its analogue within the DPWA scheme.

The further step in simplifying the theoretical analysis of the polarizational part of the spectrum is to use the approximation (20) for the generalized polarizability. Then, instead of (24), one arrives at

$$d\sigma_{\text{pol}}^{\text{B}}(\omega) \approx \frac{16}{3} \frac{\omega^4}{c^3 p_1^2} |\alpha_{\text{d}}(\omega)|^2 \int_{q_{\text{min}}}^{q_{\text{max}}} \frac{dq}{q} |G^{\text{HF}}(\omega, q)|^2. \quad (25)$$

To check the validity of the proposed method in [61, 63, 66] the polarizational part of the spectrum for was calculated for 0.25 - 10 keV electrons on Ba, La and Eu using the exact Born formula (24) and the approximate one (25). In all cases considered the results are close. Figure 5 illustrates this for the collision of a 250 eV electron with Ba. The discrepancy between the solid curve, corresponding to (24) with $\alpha(\omega, q)$ calculated within the RPAE, and the short-dashed one, representing (25) where the correlations were accounted for in the factor $\alpha_{\text{d}}(\omega)$ only, is almost negligible. For the sake of comparison, we also present the polarizational cross section calculated via (24) but with $\alpha(\omega, q)$ obtained in the Hartree-Fock approximation (dotted curve).

Another possibility to deduce $\alpha(\omega, q)$ is to combine (20) with (4). Provided the dependence $\sigma_{\gamma}(\omega)$ is known over a sufficiently wide ω -region one can restore the real part of $\alpha_{\text{d}}(\omega)$ from the dispersion relation. Such a way of obtaining $\alpha(\omega, q)$ is especially useful when direct calculations are difficult to perform (for example, when the BrS

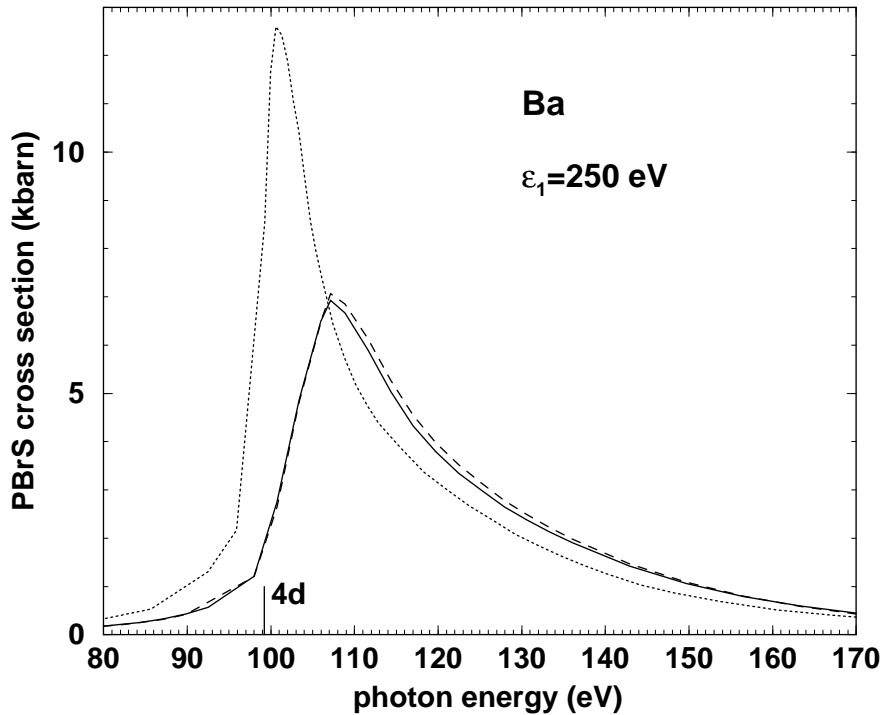


Figure 5. Polarizational BrS cross section $d\sigma_{\text{pol}}(\omega)$ for $e^- + \text{Ba}$ in the vicinity of the 4d ionization potential (marked with the vertical line). The solid curve was calculated using the exact Born formula (24), the dashed curve corresponds to (25). The dotted line originates from (24) but with $\alpha(\omega, q)$ within the Hartree-Fock approximation. [61, 66]

process is investigated in a dense media rather than in a pure ‘one electron – one atom’ collision).

To illustrate this approach in figure 6 the experimentally measured emission spectra for 500 eV electrons on La [117] are compared with the theoretical results [63, 68]. The experiment was carried out with the metallic La, therefore, the use of $\alpha(\omega, q)$ (or $\alpha_d(\omega)$) calculated for an isolated La atom seems not a fully adequate approach. To avoid this problem in [68] the experimental data for the photoabsorption spectrum [148, 149] was used to calculate the dynamic dipole polarizability, which then was substituted into (25). The factor $G^{\text{HF}}(\omega, q)$ was calculated in the Hartree-Fock approximation. The experimental data [117] have no absolute scale, so it was normalized to the magnitude of theoretical curve at the maximum. The background radiation, i.e. the ordinary BrS, was subtracted from the measured spectrum. Therefore, the experimental curve in the figure represents by itself a sum of the polarizational and the interference terms.

The agreement between the two curves is quite good. The main discrepancy is seen on the right wing of the spectrum where the experimental curve lies higher than the calculated one. This discrepancy may be attributed to the contribution of the interference term which was omitted in the calculations.

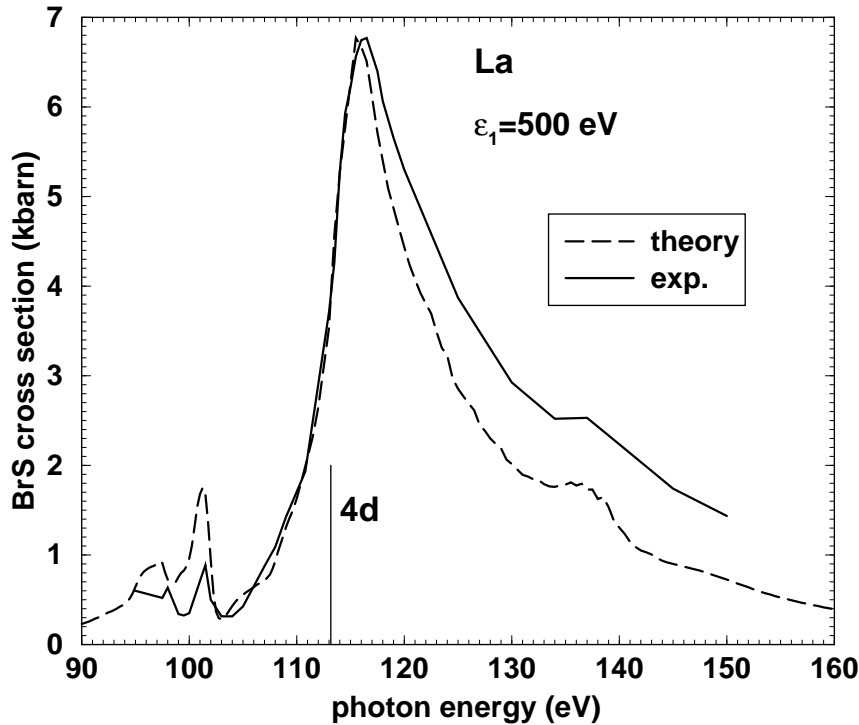


Figure 6. Comparison of experimentally measured (dashed curve) [117] BrS cross section formed in the collision of 500 eV electrons with La with the calculated dependence (solid curve) [63,68]. See also the explanation in the text.

4. BrS in collisions of heavy particles.

In this section we present the formalism and the results of numerical calculations of the BrS spectra formed in a collision of two heavy particles. We restrict ourselves to the case of ‘fast’ collisions, when the translational motion of the colliders can be described by plane waves. The peculiar features of the BrS formed in slow collisions, and, in particular, its relationship to the well-known molecular orbital radiation, are discussed in [75].

Let us describe in short the formalism which allows one to calculate the BrS spectrum formed in fast non-relativistic collisions of two atomic particles. Following the papers [34,35], where such a problem was solved for the first time, we consider the general case when both colliders, a projectile and a target, have internal dynamic structure. In what follows we use the term ‘atom 1’ for a projectile, and ‘atom 2’ for a target.

Let $M_{1,2} \gg 1$ denote the masses of the atoms, $Z_{1,2}$ stand the charges of the nuclei, $\mathbf{p}_{1,2}$ and $\mathbf{p}'_{1,2}$ notate the translation momenta before and after the collision, respectively. Apart from the translation momentum the state of each particle is characterized by the set of quantum numbers which refer to its internal (electronic) state. We assume that both atoms before and after the collision are in their grounds

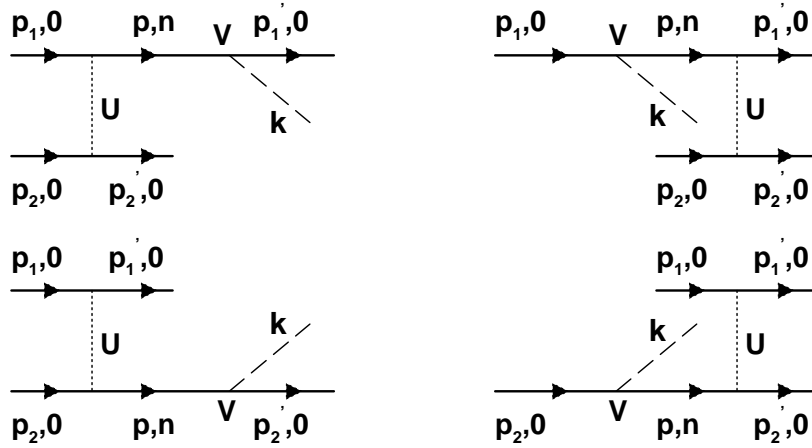


Figure 7. Diagrammatical representation of the BrS amplitude in an atom-atom collision.

states which are notated with '0'. The interaction between the atoms is described by the potential $\hat{U} \equiv U(\{\mathbf{r}\}_1, \{\mathbf{r}\}_2)$ (here $\{\mathbf{r}\}_j$, $j = 1, 2$, denote the coordinates of all the particles in atom '1' and atom '2'), which is the sum of the pair interactions between the constituents of the two atoms. For each one of the colliders the interaction with the field of radiation is described by the operator V which has the general form $\hat{V} = \sum_{i=1}^N (e_i/m_i) \exp(-i\mathbf{k}\mathbf{r}_i) (\mathbf{e}\hat{\mathbf{p}}_i)$. Here the sum is carried out over the atom's constituents of the total number N , the quantities e_i and m_i stand for the charges and the masses of the constituents, and $\hat{\mathbf{p}}_i$ is the momentum operator.

In the lowest orders of the perturbation theory in U and V the process of photon emission is represented by four diagrams drawn in figure (7). The solid lines denote the atoms, the dashed lines stand for the emitted photon, whose momentum is \mathbf{k} , energy ω and polarization \mathbf{e} , the vertical dotted lines represent the interaction \hat{U} . The two upper diagrammes correspond to the photon emission by a projectile which is virtually polarized by the target. The amplitude of this process is written as follows:

$$f_1 = \int \frac{d\mathbf{p}}{(2\pi)^3} \sum_n \left[\frac{\langle \mathbf{p}'_1, 0 | \hat{V} | \mathbf{p}; n \rangle \langle \mathbf{p}, n; \mathbf{p}'_2, 0 | \hat{U} | \mathbf{p}_1, 0; \mathbf{p}_2, 0 \rangle}{\varepsilon_n - \varepsilon_0 + E_{\mathbf{p}} - E_{\mathbf{p}_1} + E_{\mathbf{p}'_2} - E_{\mathbf{p}_2}} + \frac{\langle \mathbf{p}'_1, 0; \mathbf{p}'_2, 0 | \hat{U} | \mathbf{p}, n; \mathbf{p}_2, 0 \rangle \langle \mathbf{p}, n | \hat{V} | \mathbf{p}_1; 0 \rangle}{\varepsilon_n - \varepsilon_0 + \omega + E_{\mathbf{p}} - E_{\mathbf{p}_1}} \right]. \quad (26)$$

Here $E_{\mathbf{p}} = p^2/2M$ stands for the kinetic energy of the translation motion, ε denotes the energy of the electronic state of the projectile, the integration is carried out over the translation momentum of the projectile in the intermediate (virtual) state, and the sum \sum_n is evaluated over the whole spectrum (including the excitations into the continuum) of the internal degrees of freedom of the atom 1.

The process of the photon emission by the target, is described by the lower pair of diagrammes, and defines the amplitude f_2 . The analytic expression for f_2 one obtains from (26) by exchanging the characteristics of the atom '1' with those of the atom '2'.

The total BrS amplitude is given by

$$f = f_1 + f_2. \quad (27)$$

To evaluate the terms $f_{1,2}$ one starts with the factorization of the center-of-mass motion in the definition of the wavefunction of a complex system:

$$\Psi_{\mathbf{p}n}(\{\mathbf{r}_i\}) = e^{i\mathbf{p}\mathbf{R}}\psi_n(\{\mathbf{r}_i - \mathbf{R}\}), \quad (28)$$

where \mathbf{p} is the momentum of the center-of-mass, \mathbf{R} is its radius-vector, $\psi_n(\{\mathbf{r}_i - \mathbf{R}\})$ is the wavefunction describing the internal degrees of freedom of the system's constituents with the subscript 'n' staying for all the necessary quantum numbers.

Then, integrating over the motion of the center-of-masses of the colliders, one expresses the matrix elements $\langle \mathbf{p}', m' | \hat{V} | \mathbf{p}; m \rangle$ and $\langle \mathbf{p}'_2, m'_2; \mathbf{p}'_1, m'_1 | \hat{U} | \mathbf{p}_1, m_1; \mathbf{p}_2, m_2 \rangle$ in terms of the matrix elements between the corresponding wavefunctions ψ which describe the internal states. Finally, accounting for $v_{1,2}/c \ll 1$ ($v_{1,2}$ are the velocities of the colliders) and carrying out the dipole-photon limit $\omega(R_{\text{at}})_{1,2}/c \ll 1$ one arrives at:

$$f_1 = \frac{4\pi(\mathbf{e}\mathbf{q})}{q^2} (Z_2 - F_2(q)) A_1(\omega, q), \quad (29)$$

where $\mathbf{q} = \mathbf{p}_1 - \mathbf{p}'_1 = \mathbf{p}'_2 - \mathbf{p}_2$ is the momentum transfer. The function $A_1(\omega, q)$ is defined as follows:

$$A_1(\omega, q) = \frac{Z_1 - F_1(q)}{M_1\omega} e_1 - \omega\alpha_1(\omega, q), \quad (30)$$

where $\alpha_1(\omega, q)$ is the generalized polarizability of the projectile, and e_1 is its net charge. In (29) and (30) the quantities $F_{1,2}(q)$ are the form-factors of the atoms.

Interchanging in (29) the indices 1 and 2 one obtains the amplitude f_2 . Therefore, the total amplitude of the BrS in atom-atom scattering is

$$f = \frac{4\pi(\mathbf{e}\mathbf{q})}{q^2} \left[(Z_2 - F_2(q)) A_1(\omega, q) - (Z_1 - F_1(q)) A_2(\omega, q) \right] \quad (31)$$

This general formula generalizes the result of the Born approximation in application to the structureless charged particle scattering on a many-electron target, see (1). The right-hand side of (31) reduces to that of (1) if one considers $\alpha_1(\omega, q) = 0$ and $F_1(\omega, q) = 0$. In this limit the first term in (31) reduces to f_{ord} , whereas the second one reproduces the PBrS amplitude.

Another feature which we would like to note in connection with (31) is the vanishing of the total BrS amplitude in the collision of two identical particles. Indeed, in this case the moduli of both terms are equal and the minus sign leads to $f = 0$. This is not surprising if one recalls that (31) corresponds to the dipole-photon approximation, in whose framework any system of identical particles (no matter how complex they are) does not radiate. This restriction does not hold beyond the dipole approximation. The most rigorous treatment of the BrS problem in the non-dipolar domain should also include the consideration of the relativistic effects. The formalism describing the BrS radiation in relativistic collisions of atomic particles can be found in [39].

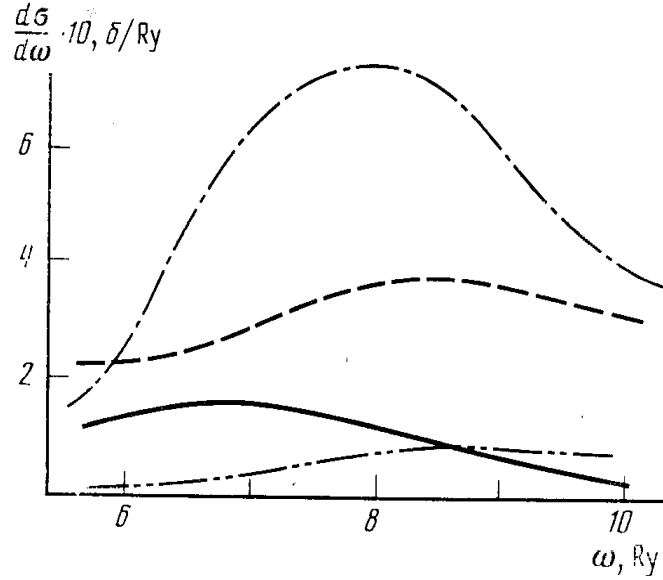


Figure 8. BrS spectral distribution (in barn/ryd) in collisions of various particles with a Xe atom [51]. Dashed line represents the total BrS spectrum for an electron, dashed-dotted line stands for $d\sigma/d\omega$ for an α -particle, dashed-double-dotted line - the spectrum for a He atom with no account for $\alpha_{\text{He}}(\omega, q)$, solid line describes the spectrum for He+Xe collision with account for $\alpha_{\text{He}}(\omega, q)$. In all cases the initial velocity of the projectile is 5 a.u.

Using the amplitude (31) one derives the following expression for the spectral distribution of the BrS radiation in atom-atom collisions:

$$\frac{d\sigma}{d\omega} = \frac{16\omega^3}{3c^3v_1^2} \int_{q_{\min}}^{q_{\max}} \frac{dq}{q} \left| (Z_2 - F_2(q)) A_1(\omega, q) - (Z_1 - F_1(q)) A_2(\omega, q) \right|^2. \quad (32)$$

Here q_{\min} and q_{\max} are the minimum and maximum momentum transfer:

$$q_{\min} = \mu v_1 \left(1 - \sqrt{1 - 2\omega/\mu v_1^2} \right), \quad q_{\max} = \mu v_1 \left(1 + \sqrt{1 - 2\omega/\mu v_1^2} \right), \quad (33)$$

and μ stands for the reduced mass of the colliders.

It was mentioned in section 2 that for the same initial velocity of the intensity of the BrS formed in the collisions of a heavy particle with a many-electron atom can be comparable or even higher that that in the electron-atom collision. To illustrate this we included figure 8 where the dependences $d\sigma/d\omega$ are presented for the collisions $e^- + \text{Xe}$, $\alpha + \text{Xe}$ and He+Xe for the range of photon energies in the vicinity of the ionization potential of the 4d subshell in Xe, $I_{4d} = 73.4$ eV. All curves correspond to the initial velocity $v_1 = 5$ a.u.

The spectra were calculated with the help of (32) the integrand of which acquires simplified forms (as was mentioned above) in the case of electron- and α -Xe collisions. The form-factors of He and Xe were calculated in the Hartree-Fock approximation, the

generalized polarizability of Xe, $\alpha_{\text{Xe}}(\omega, q)$ within the RPAE scheme as it was done in [22]. The generalized polarizability of He was approximated by $\alpha_{\text{He}}(\omega, q) \approx -F_{\text{He}}(q)/\omega^2$ (cf. (5)) since in the considered range of the photon energies (6...10 ryd) the strong inequality $\omega \gg I_{\text{He}} \approx 2$ ryd is valid. Although $|\alpha_{\text{He}}(\omega, q)|^2 \ll |\alpha_{\text{Xe}}(\omega, q)|^2$ in the range $\omega \sim I_{\text{Ad}}$, the two terms in the brackets in the integrand from (32) are of the same order of magnitude, and the interference between them is important when calculating the spectrum.

The most striking feature clearly seen in the figure is that in the whole spectral interval the magnitude of $d\sigma/d\omega$ for the collision $\alpha+\text{Xe}$ exceeds that formed in the collision $e^-+\text{Xe}$. The qualitative explanation of this effect is as follows. In the collision $e^-+\text{Xe}$ both channels, the ordinary and the polarizational, contribute to the amplitude/spectrum. The amplitude of the process is described by (1) where one uses $m = 1$ and $e = 1$. In the case of α -particle scattering, $f_{\text{ord}} \rightarrow 0$ because of a large mass of the projectile, but $f_{\text{pol}} \propto 2\alpha_{\text{Xe}}(\omega, q)$ is two times higher than for an electron. Therefore, the polarizational part of the spectrum for an α -particle is approximately four times larger than the PBrS of an electron. In the latter case, however, there are contributions of the terms $d\sigma_{\text{ord}}$ and $d\sigma_{\text{int}}$ which reduce the discrepancy.

Another important feature which is illustrated by the figure is that the intensity of the radiation in collision of a neutral and compact He atom with Xe is, in the order of magnitude, equal to that for α - and e^- -Xe collisions. This is totally due to the polarizational BrS which appears as a result of virtual polarization of Xe during the collision.

In the case of a heavy charged structureless projectile the ordinary BrS can be neglected (the first terms in (1 and in the brackets in (32))) and the spectrum is defined by the polarizational channel only. In this case (32) reduces to

$$d\sigma_{\text{pol}}(\omega, v_1) \equiv \omega \frac{d\sigma}{d\omega} = \frac{16e^2\omega^4}{3c^3v_1^2} \int_{q_{\text{min}}}^{q_{\text{max}}} \frac{dq}{q} |\alpha(\omega, q)|^2, \quad (34)$$

where e is the charge of projectile.

Various methods of calculation of the generalized polarizability $\alpha(\omega, q)$ in the ω -regions in vicinities of the ionization potentials of the atomic subshells as well as in the limit $\omega \gg I_{1s}$ have been already discussed above in the paper. Here we want to mention the approach, developed recently [69,77], which is very effective for the description of the dynamic response in the photon energy range corresponding to the ionization potentials of the the K- and L- atomic shells. In this case the electrons of these shells provide the main contribution to the polarizational BrS cross section. The method is based on the use of the non-relativistic Coulomb Green's function (see, e.g. [150]) and the hydrogen-like wave functions for the inner shell electrons calculated in the field of the effective nucleus charge Z_{eff} . The main difficulty in the description of the many-electron system in terms of the single electron hydrogen-like wave functions consists in the correct accounting for the Pauli principle. In the cited paper it was demonstrated that the Pauli principle can be taken into account by using the subtraction procedure, which cancels the electron transitions from the ground state to the occupied atomic levels. Hence,

within the framework of this approach the exact generalized polarizability $\alpha(\omega, q)$ of the inner subshell with quantum numbers n and l (the principal and the orbital quantum numbers) is approximated as follows:

$$\alpha_{nl}(\omega, q) \approx \tilde{\alpha}_{nl}(\omega, q) - \sum_{n'l'} \tilde{\alpha}_{nl \rightarrow n'l'}(\omega, q). \quad (35)$$

Here $\tilde{\alpha}_{nl}(\omega, q)$ is the generalized dynamic polarizability of the nl -state but calculated in the point Coulomb field of the charge Z_{eff} . The latter can be chosen, for example, from the condition $I_{nl} = Z_{\text{eff}}^2/2n^2$, i.e. the ionization potential is approximated by the corresponding hydrogen-like value, or one may crudely put $Z_{\text{eff}} = Z$ in the case of the K-shell electrons. The quantities n' and l' on the right-hand side of (35) are the quantum numbers of the occupied subshells in the many-electron atom the transition to which is allowed by the dipole selection rules but is forbidden by the Pauli principle. Hence, each term $\tilde{\alpha}_{nl \rightarrow n'l'}(\omega, q)$ corresponds to the contribution to $\tilde{\alpha}_{nl}(\omega, q)$ due to the discrete dipole transition $(n, l) \rightarrow (n', l')$. To meet the Pauli principle all these terms must be subtracted from $\tilde{\alpha}_{nl}(\omega, q)$.

The total polarizability of the atom is the sum of all $\alpha_{nl}(\omega, q)$. The approximation (35) fails for the subshells which exhibit a strong correlated reaction to the action of an external field. For such subshells the model of independent electrons is inapplicable. In contrast, the dynamics of electrons in the inner shells (K- and/or L-shells) is mainly governed by the action of the field of nucleus which outpowers the inter-electron correlations. Therefore, the substitution of the exact polarizability $\alpha_{nl}(\omega, q)$ with its point Coulomb analogue is justified. In many-electron atoms the ionization potentials of the K- and L-shells are well-separated. Therefore, if one is interested in the magnitude of $\alpha(\omega, q)$ in the range, for example, $\omega \sim I_K$, then one can neglect the contribution of all the shells but K to the generalized polarizability and to approximate $\alpha(\omega, q) \approx \alpha_{1s}(\omega, q) \approx \tilde{\alpha}_{1s}(\omega, q) - \sum_{n'l'} \tilde{\alpha}_{1s \rightarrow n'l'}(\omega, q)$. The analytic formulae for $\tilde{\alpha}_{nl}(\omega, q)$ and $\tilde{\alpha}_{1s \rightarrow n'l'}(\omega, q)$ are presented in [72].

In figures 9 and 10 we present the results of calculations of the PBrS cross sections in vicinities of the K-shell ionization potentials Na and Ar atoms. Full curves represent the polarizational BrS cross section (34) $\alpha(\omega, q)$ obtained in the Hartree-Fock approximation. Dotted curves represent the PBrS cross section calculated with the use of the hydrogen-like polarizability $\tilde{\alpha}_{1s}(\omega, q)$ which does not take into account the Pauli principle (see 35). For each target the effective charge Z_{eff} was chosen from the condition $Z_{\text{eff}} = Z$. The comparison of dotted and solid curves shows that the cross sections obtained in the Hartree-Fock and the purely hydrogen-like approximations have the same order of magnitude but do not agree well enough.

The discrepancy between the two models becomes less pronounced if one takes into account the Pauli principle. The results of the calculation of the PBrS cross sections in this case are plotted as broken curves which, as it is seen from the figures, reproduce the behaviour of the Hartree-Fock cross sections reasonably well. The discrepancy between the two approaches is comparable with the accuracy of the Hartree-Fock method itself. The deviation of the hydrogen approximation from the Hartree-Fock

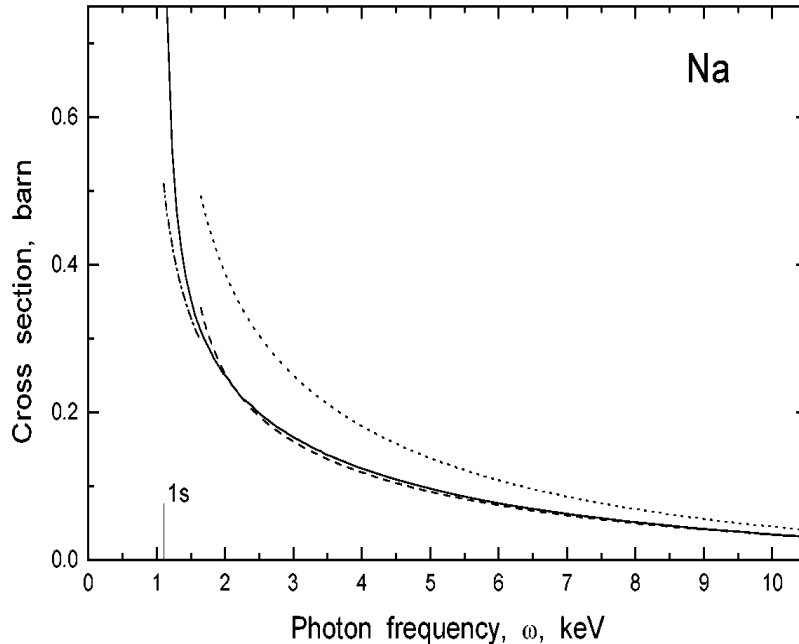


Figure 9. The PBrS cross sections $d\sigma_{\text{pol}}(\omega, v_1)$ (see (34)) for the collision of a proton with a Na atom ($Z = 11$) for the photon energies above the K-shell ionization potential (marked by a vertical line) [69]. The collision velocity is $v_1 = 40$ au. Full curve, the cross section obtained in the Hartree-Fock approximation. Dotted curve, the cross section obtained in the hydrogen-like model (with $Z_{\text{eff}} = Z$) without the Pauli principle taken into account. Broken curve, the cross section obtained in the hydrogen-like model ($Z_{\text{eff}} = Z$) with the Pauli principle taken into account. Chain curve, the cross section obtained in the hydrogen-like model (with $Z_{\text{eff}} = 9$) with the Pauli principle taken into account.

one becomes significant in the vicinity of the hydrogen-like ionization potential of the K-shell. Shifting of the hydrogen-like ionization potential of the K-shell occurs due to the inter-electron interaction. This phenomenon can be taken into account within the frame of the hydrogen-like model by choosing the value of Z_{eff} from the condition $I_{1s} = Z_{\text{eff}}^2/2$ instead of $Z_{\text{eff}} = Z$ (I_{1s} is the Hartree-Fock ionization potential of the K-shell). The PBrS cross sections calculated with this values of Z_{eff} are shown in figures by chained curves. The figures demonstrate that the imaginary continuation of the chained curves smoothly matches the broken curves in the vicinity of the hydrogen-like ionization potential. This means that the hydrogen-like approach provides a simple and effective method for the PBrS cross section calculations applicable over the whole range of photon energies above the ionization potentials of the inner atomic shells.

The use of the hydrogen-like approximation for the description of the generalized

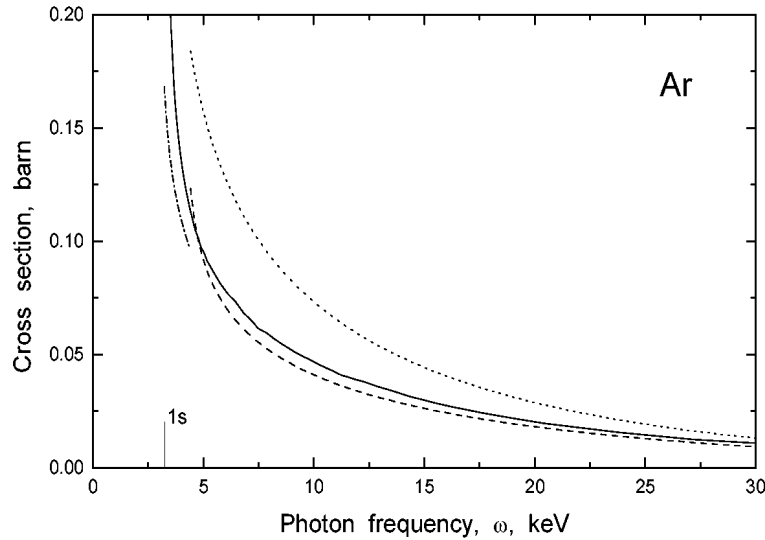


Figure 10. Same as in figure 9 but for an Ar atom ($Z = 18$). The chain curve was obtained for $Z_{\text{eff}} = 15.4$.

atomic polarizability allowed to evaluate the scaling law for the polarizational BrS cross section [69] which, for a heavy projectile, defines the total BrS cross section. In the hydrogen-like model the distance and energy can be scaled by the factors $1/Z_{\text{eff}}$ and Z_{eff}^2 respectively. Therefore, one can derive the following scaling law for the generalized polarizability $\alpha_{nl}(\omega, q)$ defined in (35):

$$\alpha_{nl}(\omega, q) = \frac{N_{nl}}{Z_{\text{eff}}^4} \alpha_{nl}^{\text{red}} \left(\frac{\omega}{Z_{\text{eff}}^2}, \frac{q}{Z_{\text{eff}}} \right), \quad (36)$$

where N_{nl} is the number of electrons in the subshell (nl), and α_{nl}^{red} denotes the expression on the right-hand side of (35) calculated for the (nl)-subshell of a hydrogen atom.

Using (36) in (34) one expresses the cross section $d\sigma_{\text{pol}}(\omega, v_1)$ calculated in the range $\omega \sim I_{nl}$ and for the projectile of velocity v_1 in terms of $d\sigma_{\text{pol}}^{\text{red}}(\omega/Z_{\text{eff}}^2, v_1/Z_{\text{eff}})$, which is the BrS cross section for the collision with a hydrogen atom but for the scaled velocity v_1/Z_{eff} and the scaled photon energy ω/Z_{eff}^2 :

$$d\sigma_{\text{pol}}(\omega, v_1) = \frac{N_{nl}^2}{Z_{\text{eff}}^2} d\sigma_{\text{pol}}^{\text{red}} \left(\frac{\omega}{Z_{\text{eff}}^2}, \frac{v_1}{Z_{\text{eff}}} \right). \quad (37)$$

In the limit of high-energy photons, $\omega \gg I_{1s}$, the generalized polarizability is expressed via the form-factor $F(q)$ (see (5)). The parameter Z_{eff} can be chosen equal to Z . Then, the PBrS cross section depends on the single parameter, $\omega/(vZ)$, and the scaling law (37) reduces to that discussed in [151].

As mentioned in section 2 there is a peculiar feature in the PBrS emitted in the collision of a fast heavy charged particle with a many-electron atom. This feature

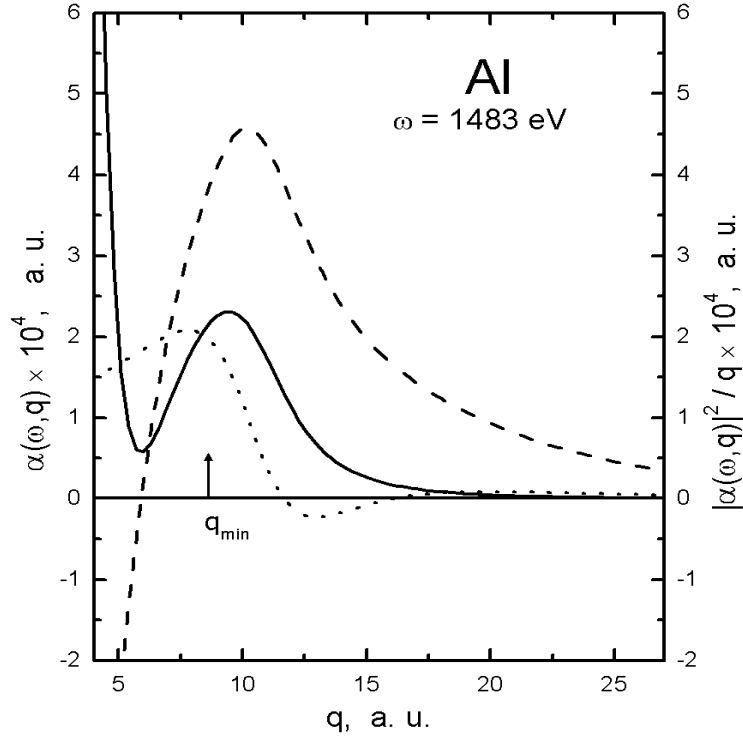


Figure 11. The q -dependence of $\alpha(\omega, q)$ of an Al atom at fixed frequency $\omega = 1483$ eV [79]. Dashed and dotted curves represent $\text{Re}[\alpha(\omega, q)]$ and $\text{Im}[\alpha(\omega, q)]$ respectively. The solid curve shows the behaviour of the integrand in (34), $|\alpha(\omega, q)|^2/q$.

originates from the kinematics of the atomic electrons in the process and manifests itself as an additional maximum in the velocity dependence of the PBrS cross section. A similar peculiarity, known as the Bethe ridge, appears in the differential cross section of the impact ionization of an atom by a charged particle [124], where there is a ridge in the dependence of the cross section on the transferred momentum q and the momentum of the outgoing electron p_e at $q \sim p_e$. This ridge in the differential cross section is a result of the momentum transfer to one of the target electrons in the collision process. The peculiarity in the polarizational BrS process arises from the similar dynamics of atomic electrons [79]. However, in this process after virtual excitation the atomic electron returns to its initial state radiating a photon. The Bethe-type virtual excitations of electrons in the PBrS process give rise to the additional maximum in the velocity dependence of the cross section.

Let us briefly outline the reasons which lead to the Bethe peculiarity in the velocity dependence of $d\sigma_{\text{pol}}(\omega, v_1)$ (the details are given in [79]). The cross section $d\sigma_{\text{pol}}(\omega, v_1)$, defined in (34), depends on the generalized polarizability $\alpha(\omega, q)$, which (in the case of a spherically-symmetric target) can be written as follows:

$$\alpha(\omega, q) = \frac{1}{(\mathbf{e}\mathbf{q})} \sum_n \left\{ \frac{\langle 0 | \mathbf{e}\hat{\mathbf{p}} | n \rangle F_{n0}(\mathbf{q})}{\omega_{n0} - \omega - i0} + \frac{F_{0n}(\mathbf{q}) \langle n | \mathbf{e}\hat{\mathbf{p}} | 0 \rangle}{\omega_{n0} + \omega} \right\}. \quad (38)$$

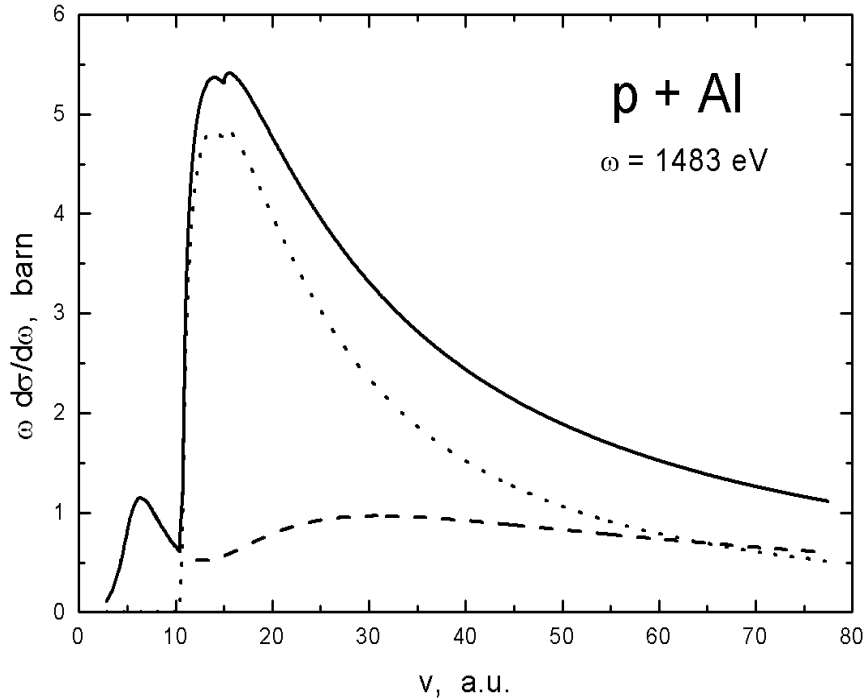


Figure 12. Velocity dependencies of the elastic PBrS (dotted curve) and inelastic PBrS (dashed curve) cross sections at $\omega = 1483$ eV. The solid curve is the total photon emission cross section as a function of v_1 [79].

The notations are explained in the paragraph after eq. (9).

The matrix element $F_{n0}(\mathbf{q}) = \langle m | \exp(i\mathbf{q}\mathbf{r}) | 0 \rangle$ in (38) as a function of the intermediate state energy ε_n is maximal if $\varepsilon_n = q^2/2$. This means that the momentum is mainly transferred to the electron in the intermediate state. Similar behaviour of matrix elements is known from electron–atom impact ionization where it is called ‘the Bethe ridge’. In the PBrS process the Bethe peculiarity results in the relationship between the photon energy and the transferred momentum:

$$\omega \approx \frac{q^2}{2} + I, \quad (39)$$

where I is the ionization potential of the subshell from which the electron is excited. This relation defines the curve in the plane (ω, q) in the vicinity of which the generalized polarizability $\alpha(\omega, q)$ as a function of q has a resonance character. This is illustrated by figure 11.

In [79] it was demonstrated that the resonant-like behavior of $|\alpha(\omega, q)|^2$ results in the peculiarity (a maximum) in the PBrS cross section $d\sigma_{\text{pol}}(\omega, v_1)$ as a function of v_1 . The Bethe peculiarity is mostly pronounced if the velocity and the photon energy satisfy the conditions $v_1 \sim \sqrt{(\omega + I)/2} < \sqrt{2\omega}$ which ensures that the elastic PBrS

dominates over the inelastic one in the total emission spectrum, and, consequently, that the contribution of inelastic channels does not smear out the peculiarity.

Figure 12 illustrates this effect. The maximum in the total emission spectrum (the solid curve) formed in $p+\text{Al}$ collision is due to the maximum of $d\sigma_{\text{pol}}(\omega, v_1)$ as a function of the velocity. In the vicinity of maximum the contribution of the inelastic channel (the dashed curve) is small.

5. Conclusions

This review was focused on the achievements made during last decade in the development of the theory of polarizational BrS formed in non-relativistic collisions of various particles with *isolated* many-electron atoms. Apart from what has been described above in the paper we would like to mention that a number of algorithms and computer codes have been developed, which allows one to perform an accurate quantitative analysis of the spectral and spectral-angular distributions of the total BrS formed in an arbitrary collision process which involves a charged structureless particle and a multi-electron complex (including molecules and clusters [90]).

However, not all of the problems related to the PBrS effect have been equally developed. Among these we mention the process of inelastic BrS, the non-dipolar effects, the role of PBrS in low-energy electron/positron-atom scattering.

The main physical reason for paying less attention to the process of inelastic BrS is that, as it was mentioned, in wide ranges of photon energies and collision velocities the contribution of the inelastic channels is parametrically smaller than that of the elastic BrS due to the coherence nature of the latter. However, the level of accuracy which can be achieved, at present, in the quantitative description of the inelastic BrS, especially in the case of electron-atom scattering, cannot be matched with that achieved for the elastic BrS process. An accurate study of the inelastic radiative scattering is a more difficult problem both from theoretical and computational points of view. Therefore there exist fewer in this field. Particular interest can be attached to the understanding of collective excitations in inelastic radiative scattering.

The discussions and numerical calculations of the PBrS beyond the dipole-photon approximation have not been as extensive as those based on the dipole-photon scheme. The non-dipolar effects include two aspects. The first one is related to the emission into higher multipoles. Its relative significance, which is governed by the magnitude of the factor kR_{at} ($k = \omega/c$ is the momentum of the photon), increases with the photon energy ω . Therefore, if one is interested in the accurate data on the PBrS characteristics in the range of photon energies higher than several keV, the corrections to the dipole-photon approximation must be accounted for. The non-dipolar effects manifests themselves in PBrS also via the retardation in the interaction between the projectile and the target's electrons. The retardation modifies the Coulomb interaction adding the terms proportional to v_1/c (v_1 is the velocity of the projectile). These terms become noticeable for electrons of kinetic energy of several tens of keV. We note that within this energy

range the latest experiments on the detection of PBrS were performed [59]. Both of these effects, the emission into higher multipoles and the retardation, are incorporated in the full relativistic theory of PBrS developed recently [85, 86].

Finally, we mention the problem of the role of PBrS mechanism in a low-energy ($\varepsilon_1 < I_1$) electron–atom collision. In this case the polarization of the target can influence the radiation process not only via the PBrS mechanism directly but in a less evident way. Namely, the dynamically induced dipole moment may lead to the modification of the projectile’s wavefunction (more precisely, the phaseshifts). This will influence the amplitude of the *ordinary* BrS. This effect, which will be mostly pronounced for the targets with large dipole polarizabilities, has not been studied in detail so far.

The above described processes do not cover all the phenomena which are worth to be investigated further. The polarizational BrS problem is rather broad, because this kind of radiation can be emitted in any collision involving structured particles: nuclei, atoms, molecules or clusters. The number of various colliding pairs, different interaction forces between particles, kinematical conditions and the frequency ranges make this problem quite varied and interesting.

Acknowledgments

This work is supported by the Russian Foundation for Basic Research (Grant No 96-02-17922-a) and INTAS (Grant No 03-51-6170). AVK acknowledges the support of the Alexander von Humboldt Foundation.

References

- [1] Akhiezer, A. I. and Berestetsky, V. B., 1981. Quantum Electrodynamics. Nauka, Moscow.
- [2] Tsytoich, V. N., Ojringel, I. M. (Eds.) 1993. Polarizational bremsstrahlung. Plenum, NY.
- [3] Pratt R.H., 1981. Comments At. Mol. Phys. 10, 121-131.
- [4] Koch, H. W., Motz, J. W., 1959. Rev. Mod. Phys. 116, 920.
- [5] Pratt, R.H., 1984. In: Lutz H.O., Briggs J.S. and Kleinpoppen H. (Eds.), Fundamental Processes in Energetic Atomic Collisions, Plenum, NY, pp. 145-182.
- [6] Pratt, R. H., Feng, I. J., 1985. In: Craseman B. (Ed.), Atomic Inner-Shell Physics, Plenum, NY, Ch. 12, pp. 533-580.
- [7] Nakel, W. 1994. Phys. Rep. 243, 317.
- [8] Pratt, R. H., Shaffer, C. D., Avdonina, N. B., Tong, X.-M., Florescu, V., 1995. Nucl. Instrum. Methods B 99, 156-159.
- [9] Pratt, R. H., Tseng, H. K., Lee, C. M., Kissel, L., MacCallum, C., Riley, M., 1977. At Data Nucl. Data Tables 20, 175-209 (Erratum: 1981. ibid. 26, 477-481).
- [10] Kissel, L., Quarles, C. A., Pratt, R. H., 1983. At. Data Nucl. Data Tables 28, 381.
- [11] Buimistrov, V.M., Trakhtenberg, L. I., 1975. Sov. Phys. – JETP 42, 54.
- [12] Amusia, M. Ya., Baltenkov, A. S., Paiziev, A. A., 1976. Sov. Phys. – JETP Lett. 24, 332-334.
- [13] Pindzola, M. S., Kelly, H. P., 1976. Phys. Rev. A 14, 204-210.
- [14] Amusia, M. Ya., Baltenkov, A. S., Gilerson, V.B., 1977. Sov. Phys. – Tech. Phys. Lett. 3, 455.
- [15] Buimistrov, V.M., Trakhtenberg, L. I., 1977. Sov. Phys. – JETP 46, 447.
- [16] Wendin, G., Nuroh K., 1977. Phys. Rev. Lett. 39, 48.
- [17] Zon, B. A., 1977. Sov. Phys. – JETP 46, 65.

- [18] Zon, B. A., 1979. *Sov. Phys. – JETP* 50, 23.
- [19] Golovinski, P. A., Zon, B. A., 1980 *Sov. Phys. Tech. Phys.* 25, 1076.
- [20] Zimkina, T. M., Shulakov, A. S., Brajko, A. P., 1981. *Fiz. Tverd. Tela* 23, 2006.
- [21] Amusia M. Ya., Zimkina T. M., Kuchiev M. Yu., 1982. *Sov. Phys. - Tech. Phys.* 27, 866.
- [22] Amusia, M. Ya., Avdonina, N. B., Chernysheva, L. V., Kuchiev, M. Yu., 1985. *J. Phys. B* 18, L791-L796.
- [23] Verkhovtseva, E. T, Gnatchenko, E. V., Pogrebnyak, P. S., 1983. *J. Phys. B* 16, L613-L616.
- [24] Amusia, M. Ya., Avdonina, N. B., Kuchiev, M. Yu., Chernysheva, L. V., 1986. *Izv. Acad. Nauk SSSR: Ser. Fiz.* 50, 1261-1266.
- [25] Avdonina, N. B., Amusia, M. Ya., Kuchiev, M. Yu., Chernysheva, L. V., 1986. *Sov. Phys. – Tech. Phys.* 31, 150-155.
- [26] Amusia, M. Ya., Chernysheva, L. V., Korol, A. V., 1990. *J. Phys. B* 23, 2899-2907.
- [27] Amusia, M. Ya., Korol, A. V., 1991. *J. Phys. B* 24, 3251-3265.
- [28] Amusia, M. Ya., Kuchiev, M. Yu., Korol, A. V., Solov'yov, A. V., 1985. *Sov. Phys. - JETP* 61, 224-228.
- [29] Astapenko, V. A., Buimistrov, V. M., Krotov, Yu. A., Mihailov, L. K., Trakhtenberg, L. I., 1985. *Sov. Phys. – JETP* 61, 930.
- [30] Buimistrov, V. M., Krotov, Yu. A., Trakhtenberg, L. I., 1980. *Sov. Phys. - JETP* 52, 411.
- [31] Ishii, K., Morita, S., 1984. *Phys. Rev. A* 30, 2278;
- [32] Ishii, K., Morita, S., 1985. *Phys. Rev. A* 31, 1168.
- [33] González, A. D., Miraglia, J. E., Garibotti, C. R., 1988. *Phys. Rev. A* 34, 2834-2841.
- [34] Amusia, M. Ya., Kuchiev, M. Yu., Solov'yov, A. V., 1984. *Sov. Phys. - Tech. Phys. Lett.* 10, 431-432.
- [35] Amusia, M. Ya., Kuchiev, M. Yu., Solov'yov, A. V., 1985. *Sov. Phys. – JETP* 62, 876-881.
- [36] Amusia, M. Ya., Solov'yov, A. V., 1990. *J. Phys. B* 23, 2889-2898.
- [37] Amusia, M. Ya., Kuchiev, M. Yu., Solov'yov, A. V., 1987. *Sov. Phys. - Tech. Phys.* 32, 499-500.
- [38] Amusia, M. Ya., Kuchiev, M. Yu., Solov'yov, A. V., 1988. *Sov. Phys. – JETP* 67, p.41-48.
- [39] Amusia, M. Ya., Solov'yov, A. V., 1990. *Sov. Phys. – JETP* 70, 416-425.
- [40] Dubois, A., Maquet, A., Jetzke, S., 1986. *Phys. Rev. A* 34, 1888-1895.
- [41] Dubois, A., Maquet, A., 1989. *Phys. Rev. A* 40, 4288-4297.
- [42] Amusia, M. Ya., Solov'yov, A. V., 1985. *J. Phys. B* 18, 3663-3666.
- [43] Amusia, M. Ya., Gribakin, G. F., Kharchenko, V. A., Korol, A. V., Solov'yov, A. V., 1988. *Muon Cat. Fusion* 2, 143-146.
- [44] Amusia, M. Ya., Korol, A. V., Solov'yov, A. V., 1986. *Zeit. fur Physik D* 1, 347-349.
- [45] Amusia, M. Ya., Baltenkov, A. S., Zhalov, M. B., Korol, A. V., Solov'yov, A. V., 1986. *Polarisational bremsstrahlung in scattering of particles at atoms and nuclei.- Proceedings of 21st Winter School of Leningrad Institute of Nuclear Physics, pp.135-194 (in Russian).*
- [46] Amusia, M. Ya., Baltenkov, A. S., Korol, A. V., Solov'yov, A. V., 1987. *Sov. Phys. – JETP* 66, 877-883.
- [47] Varfolomeev, A. A., 1978. *Yad. Fizika* 28, 1034-1039.
- [48] Varfolomeev, A. A., 1980. *Yad. Fizika* 31, 1268-1275.
- [49] Amusia, M. Ya., Solov'yov, A. V., 1987. In: Sushkov, O. P. (ed.), *Modern Developments in Nuclear Physics*, World Scientific, Singapore, pp. 425-437.
- [50] Solov'yov, A. V., 1989. In: Dalgarno, A., Freund R. S., Lubell, M. S., Lucatorto, T. B. (Eds.), *16th ICPEACS, Book of Abstracts.*
- [51] Amusia, M. Ya., Kuchiev, M. Yu., Solov'yov, A. V., 1985. *Sov. Phys. - Tech. Phys. Lett.* 11, 577-579.
- [52] Amusia, M. Ya., Korol, A. V., Solov'yov, A. V., 1986. *Sov. Phys. – Tech. Phys. Lett.* 12, 290-292.
- [53] Astapenko, V. A., Buimistrov, V. M., Krotov, Yu. A., 1987. *Sov. Phys. – JETP* 66, 470.
- [54] Amusia, M. Ya., 1988. *Phys. Rep.* 142, 269-335.
- [55] Amusia, M. Ya., 1990. *Bremsstrahlung. Energoatomizdat, Moscow (in Russian).*

- [56] Verweyen, A., Guthöhrlein, G. R., Gerhard E, et.al., 1996. In 17th Int. Conf. X-Ray and Inner-Shell Processes (Hamburg), Abstracts p. 170.
- [57] Quarles, C. A., 1998. Private communication.
- [58] Quarles, C. A., Portillo, S., 1999. In: Duggan, J. J., I.L.Morgan, I. L., Applications of Accelerators in Research and Industry, AIP Press, pp. 174-177.
- [59] Portillo, S., C. A. Quarles, C. A., 2003. Phys. Rev. Lett. 91, 173201.
- [60] Korol, A. V., Lyalin, A. G., Solov'yov, A. V., 1995. J. Phys. B 28, 4947-4962
- [61] Korol, A. V., Lyalin, A. G., Solov'yov, A. V., 1996. Phys. Rev. A 53, 2230-2238.
- [62] Korol, A. V., Lyalin, A. G., Solov'yov, A. V., 1996. In: Selected Topics on Electron Physics. Campbell, D. M., Kleinpoppen, H. (Eds.) Plenum, NY. pp. 263-278.
- [63] Korol, A. V., Lyalin, A. G., Solov'yov, A. V., Shulakov, A. S., 1996. JETP 82, 631-638.
- [64] Gerchikov, L. G., Korol, A. V., Lyalin, A. V., Solov'yov, A.V., 1997. In: Johnson, R. L., Schmidt-Böcking, H., Sonntag, B. F. (Eds.) AIP Conference Proceedings 389. AIP Press, pp. 447-464
- [65] Korol, A. V., 1992. J. Phys. B 25, L341-L344.
- [66] Korol, A. V., Lyalin, A. G., Solov'yov, A. V., Shulakov, A. S., 1995. J. Phys. B 28, L155-L160.
- [67] Korol, A. V., Lyalin, A. G., Solov'yov, A. V., Shulakov, A. S., 1996. J. Electron Spectr. Related Phenomena 79, 323-326.
- [68] Korol, A. V., Lyalin, A. G., Solov'yov, A. V., Shulakov, A. S., 1996. J. Phys. B 29, L611-L617.
- [69] Korol, A. V., Obolensky, O. I., Solov'yov, A. V., 1998. J. Phys. B 31, 5347-5353.
- [70] Korol, A. V., Lyalin, A. G., Solov'yov, A. V., 1999. In XX1 ICPEAC, Book of Abstracts (Sendai, Japan), p. 240.
- [71] Korol, A. V., Lyalin, A. G., Solov'yov, A. V., 1997. J. Phys. B 30, L115-L121.
- [72] Korol, A. V., Lyalin, A. G., Obolensky, O. I., Solov'yov, A. V., 1998. JETP 1998 87, 251-259.
- [73] Korol, A. V., Lyalin, A. G., Solov'yov, A.V., 1999. Opt. Spectrosc. 86, 486.
- [74] Korol, A. V., Lyalin, A. G., Solov'yov, A. V., Avdonina, N. B., Pratt, R. H., 2002. J. Phys. B 35, 1197-1210.
- [75] Solov'yov, A. V., 1992. Zh. Phys. D 24, 5.
- [76] Korol, A. V., Kuchiev, M. Yu., Solov'yov, A. V., 1992. J. Phys. B 25, 3379-3392.
- [77] Korol, A. V., Obolensky, O. I., Solov'yov, A. V., 1999. Techn. Phys. 44, 1135-1141.
- [78] Korol, A. V., 1994. J. Phys. B 27, 4765-4777.
- [79] Korol, A. V., Lyalin, A. G., Obolensky, O. I., Solov'yov, A. V., 2000. J. Phys. B 33, L179-L186.
- [80] Amusia, M. Ya., Korol, A. V., 1994. Phys. Lett. A 186, 230-234.
- [81] Connerade, J. P., Solov'yov, A. V., 1996. J. Phys. B 29, 3529-3547.
- [82] Gerchikov, L. G., Ipatov, A. N., Solov'yov, A. V., 1996. J. Phys. B 30, 5939-5959.
- [83] Gerchikov, L. G., Solov'yov, A. V., 1997. Z. Phys. D 42, p. 279-287.
- [84] Gerchikov, L. G., Ipatov, A. N., Solov'yov, A. V., 1996. J. Phys. B 31, 2331-2341.
- [85] Korol, A. V., Obolensky, O. I., Solov'yov, A. V., Solovjev, I. A., 2001. J. Phys. B 34, 1589-1617.
- [86] Korol, A. V., Lyalin, A. G., Obolensky, O. I., Solov'yov, A. V., Solovjev, I. A., 2002. JETP 94, 704-719.
- [87] Korol, A. V., Obolensky, O. I., Solov'yov, A. V., Solovjev, I. A., 2002. Surface Review and Letters 9, 1191-1195.
- [88] Korol, A. V., Solov'yov, A. V., 1997. J. Phys. B 30, 1105-1150.
- [89] Korol, A. V., Lyalin, A. G., Solov'yov, A. V., 2004. Polarizational Bremsstrahlung. Technical University Press, St. Petersburg (in Russian).
- [90] Lyalin, A. G., Solov'yov A. V., 2005. Radiat. Phys. Chem. this issue.
- [91] Korol, A. V., Solov'yov A. V., 2005. Radiat. Phys. Chem. this issue.
- [92] Astapenko, V. A., Kukushkin, A. B., 1997. JETP 84, 229-240.
- [93] Astapenko, V. A., 1999. JETP 88, 889-895.
- [94] Astapenko, V. A., Bureeva, L. A., Lisitsa, V. S., 2000. JETP 90, 434-446; *ibid.* 788-794.
- [95] Astapenko, V. A., Bureeva, L. A., Lisitsa, V. S., 2000. JETP 90, 788-794.
- [96] Astapenko, V. A., Bureeva, L. A., Lisitsa, V. S., 2000. Laser Phys. 10, 960.

- [97] Astapenko, V. A., Bureeva, L. A., Lisitsa, V. S., 2000. Phys. Scripta T86, 62-67.
- [98] Astapenko, V. A., 2001. Plasma Physics Reports 27, 474-479.
- [99] Kogan, V. I., Kukushkin, A. B., Lisitsa, V. S., 1992. Phys. Rep. 1992, 213 1.
- [100] Astapenko, V. A., Bureeva, L. A., Lisitsa, V. S., 2002. Phys. Usp. 45, 149-184.
- [101] Astapenko, V. A., 2003. Polarizational and Interference Effects in Radiative Processes. URSS, Moscow (in Russian).
- [102] Blazhevich, S.V., Cherpunov, A.S., Grishin, V.K., et. al., 1996. Phys. Lett. A 211, 309-312.
- [103] Nasonov, N. N., 1998. Nucl. Instrum. Methods B 1998 145, 19-24.
- [104] Blazhevich, S.V., Cherpunov, A.S., Grishin, V.K., et. al., 1999. Phys. Lett. A 254, 230-232.
- [105] Kamyshanchenko, N., Nasonov, N., Pokhil, G., 2001. Nucl. Instrum. Methods B 173, 195-202.
- [106] Astapenko, V. A., Buimistrov, V. M., Krotov, Yu. A., Nasonov, N. N., 2004. Phys. Lett. A 332, 298-302.
- [107] Golovinski, P. A., 1988 Sov. Phys. – JETP 67, 153.
- [108] Amusia M.Ya., Korol A.V. 1993. Nucl. Instrum. Methods B79, 146-149.
- [109] Kracke, G., Alber, G., Briggs, J. S., Maquet, A., 1993. J. Phys. B 1993, 26 L561-L566.
- [110] Kracke, G., Alber, G., Briggs, J. S., Maquet, A., Vénard V. 1994. J. Phys. B 27 3241-3256.
- [111] Amusia, M.Ya., 1990. Atomic photoeffect. Plenum, New York.
- [112] Liefeld, R. J, Burr, A. F., Chamberlain, M. B., 1974. Phys. Rev. A 9, 316-322.
- [113] Chamberlain, M. B., Burr, A. F., Liefeld, R. J, 1974. Phys. Rev. A 9, 663-667.
- [114] Berestetskii, V. B., Lifshitz, E. M., Pitaevskii L. P., 1989. Quantum Electrodynamics. Nauka, Moscow.
- [115] Shulakov, A. S., Zimkina, T. M., Brajko, A. P., et. al., 1983. Fiz. Tverd. Tela. 25, 789-795.
- [116] Zimkina, T. M., Shulakov, A. S., Brajko, A. P., et. al., 1984. Izv. Akad. Nauk SSSR, fiz. ser. 48, 1263-1272.
- [117] Zimkina, T. M., Shulakov, A. S., Brajko, A. P., et. al., 1984. Sov. Phys. – Solid State 26, 1201.
- [118] Verkhovtseva, E. T., Gnatchenko E.V., Zon B.A. et. al., 1990. Sov. Phys. JETP 71, 463.
- [119] Romanikhin, V.P., 2002. JETP 94, 239-243.
- [120] Avdonina, N. B., Pratt, R. H., 1999. J. Phys. B 32, 4261-4276.
- [121] A. A. Ratzig, A. A., Smirnov, B. M., 1908. Reference Data on Atoms, Molecules and Ions. Springer, Berlin.
- [122] Hammer, D., Frommhold, L., 2001. Phys. Rev. A 64, 024705 (Erratum: 2001. ibid. 64, 059901(E))
- [123] Greiner, W., Reinhardt, J., 1985. In: Bromley, D. A. (Ed.), Treatise on Heavy-Ion Science, vol. 5. Plenum, NY.
- [124] Landau, L. D., Lifshitz, E. M., 1965. Quantum mechanics. Pergamon, Oxford.
- [125] Zon, B. A., 1995. Zh. Exp. Teor. Phys. 107, 1176.
- [126] Tkachenko, A.A., Gnatchenko, E.V., Verkhovtseva, E.T., 1995. Opt. Spectrosc. 78, 183.
- [127] Gnatchenko, E. V., Tkachenko, A. A., Verkhovtseva E. T., 2002. Opt. Spectrosc. 92, 13-16.
- [128] Gnatchenko, E. V., Tkachenko, A. A., Verkhovtseva E. T., 2002. Surface Review and Lett. 9, 651-654.
- [129] Lee, C. M., Kissel, L., Pratt, R.H., Tseng, H.K., 1976. Phys. Rev. A 13, 1714-1727. (Erratum: 1981. ibid. 24, 2866-2867.)
- [130] Avdonina, N. B., Pratt, R. H., 1995. Nucl. Instr. Meth. 99, 166-169.
- [131] Kim, L., Pratt, R. H., 1987. Phys. Rev. A 36, 45.
- [132] Florescu, A., Obolensky, O. I., Pratt, R. H., 2002. J. Phys. B 35, 2911-2925.
- [133] Zhdanov, V. P., 1978. Fizika Plazmi 4, 128-133 (in Russian).
- [134] Tseng, H.K., 1989. Phys. Rev. A 39, 1012-1015; ibid. 40, 6826-6830.
- [135] Tseng, H. K., Pratt, R. H., 1971. Phys. Rev. A, 3, 100-115.
- [136] Shaffer, C. D., Pratt, R. H., 1997. Phys. Rev. A 56, 3653-3658.
- [137] Tseng, H. K., 1997. J. Phys. B 30, L317-L321 (Corrigendum: 2000. ibid. 33, 1471).
- [138] Keller, S., Dreizler, R. M., 1997. J. Phys. B 30, 3257-3266.
- [139] Amusia, M. Ya., Korol A. V., 1989. J. Phys. B 22 L571-L573.

- [140] Amusia, M. Ya., Korol A. V., 1992. *J. Phys. B* 25, 2383-2392.
- [141] Kurkina, L. I., 2004. *Phys. Sol. State* 46, 557-562.
- [142] Kurkina, L. I., 2004. *J. Phys. B* 37, 2649-2660.
- [143] Gonzalez, A. D., Pacher, M. C., Miraglia, J. E., 1988. *Phys. Rev. A* 37, 4974-4977.
- [144] Solov'yov, A. V., 1995. 5 EPS Conf. on At.Mol.Phys. Edinburgh, UK. Abstracts p. 711
- [145] Sobelman, I. I. 1979. *Atomic Spectra and Radiative Transitions*. Springer, Berlin.
- [146] Becker, U., Kerkhoff, H. G., Lindle, D. W., et. al., 1986. *Phys. Rev. A* 34, 2858-2864.
- [147] Amusia, M. Ya., Dolmatov, V. K., Ivanov, V. K., 1983. *Sov. Phys. – JETP* 58, 67.
- [148] Zimkina, T. M., Gribovskii, S., 1971. *J. Physique Coll. C-4, Suppl.* 10, 32, C4-282.
- [149] Henke, B. L., Gullikson, E. M., Davis, J. C., 1993. *At. Data Nucl. Data Tables* 54, 2.
- [150] Zapryagaev, S. A., Manakov, N. L., Palchikov, V. G., 1985. *The Theory of One- and Two-Electron Multicharged Ions*. Energoatomizdat, Moscow (in Russian).
- [151] Ishii, K., Morita, S., 1986. *Nucl. Instrum. Methods. B* 22, 68.